Classical Length-5 Pattern-Avoiding Permutations

Nathan Clisby

Department of Mathematics,
Swinburne University of Technology,
Hawthorn, Vic. 3122, Australia

nclisby@swin.edu.au

Andrew R. Conway

Fairfield, Vic. 3078, Australia

andrewpermutations5@greatcactus.org

Anthony J. Guttmann

School of Mathematics and Statistics
The University of Melbourne
Vic. 3010, Australia

guttmann@unimelb.edu.au

Yuma Inoue

Google Japan, SHIBUYA STREAM,
3-21-3 Shibuya, Shibuya-ku,
Tokyo 150-0002, Japan

yumai@google.com

Abstract

We have made a systematic numerical study of the 16 Wilf classes of length-5 classical pattern-avoiding permutations from their generating function coefficients. We have extended the number of known coefficients in fourteen of the sixteen classes. Careful analysis, including sequence extension, has allowed us to estimate the growth constant of all classes, and in some cases to estimate the sub-dominant power-law term associated with the exponential growth.

In six of the sixteen classes we find the familiar power-law behaviour, so that the coefficients behave like $s_n \sim C \cdot \mu^n \cdot n^g$, while in the remaining ten cases we find a stretched exponential as the most likely sub-dominant term, so that the coefficients behave like $s_n \sim C \cdot \mu^n \cdot \mu_1^{n^\sigma} \cdot n^g$, where $0 < \sigma < 1$. We have also classified the 120 possible permutations into the 16 distinct classes.

We give compelling numerical evidence, and in one case a proof, that all 16 Wilf-class generating function coefficients can be represented as moments of a non-negative measure on $[0, \infty)$. Such sequences are known as *Stieltjes moment sequences*. They have a number of nice properties, such as log-convexity, which can be used to provide quite strong rigorous lower bounds.

Stronger bounds still can be established under plausible monotonicity assumptions about the terms in the continued-fraction expansion of the generating functions

implied by the Stieltjes property. In this way we provide strong (non-rigorous) lower bounds to the growth constants, which are sometimes within a few percent of the exact value.

Mathematics Subject Classifications: 05C88, 05C89

1 Introduction

Let π be a permutation on $[n]$ and τ be a permutation on $[k]$. τ is said to occur as a *pattern* in π if for some sub-sequence of π of length k all the elements of the sub-sequence occur in the same relative order as do the elements of π. If the permutation τ does not occur in π, then this is said to be a *pattern-avoiding permutation* or PAP.

Let $s_n(\tau)$ denote the number of permutations of $[n]$ that avoid the pattern τ. Stanley and Wilf conjectured, and Marcus and Tardos [31] subsequently proved, that for any pattern τ in $[k]$ the limit $\lim_{n\to\infty} s_n(\tau)^{\frac{1}{n}}$ exists and is finite. This means that the number of PAPs grows exponentially with n, whereas of course the number of permutations of n grows factorially.

There are 6 possible permutations of length three, and the number of permutations of length n avoiding any of these 6 patterns is given precisely by $C_n = \frac{1}{n+1}\binom{2n}{n} \sim \frac{4^n}{\sqrt{\pi n^3}}$, where C_n denotes the nth Catalan number. That is to say, all 6 possible patterns have the same exponential growth-rate as PAPs. Alternatively expressed, there is only one Wilf class for length-3 PAPs.

For length-4 PAPs there are three Wilf classes. Typical representatives of the three classes are 1234, 1342 and 1324. The generating function for the first two classes is known.

In the first case [16] the generating function is D-finite, satisfying a third-order linear, homogeneous ODE, and $s_n(1234) \sim \frac{81\sqrt{3}\cdot 9^n}{16\pi\cdot n^4}$.

In the second case [6] the generating function is algebraic, and $s_n(1342) \sim \frac{64\cdot 8^n}{243\sqrt{\pi}\cdot n^{5/2}}$.

The third case has not been solved, but extensive numerical work [11] suggests that $s_n(1324) \sim C\cdot\mu^n\cdot\mu_1^{\sqrt{n}}\cdot n^g$, where $\mu \approx 11.598$ (and possibly $9+3\sqrt{3}/2$ exactly), $\mu_1 \approx 0.040$, and $g \approx -1.1$. The appearance of the sub-dominant term $\mu_1^{\sqrt{n}}$ is referred to as a *stretched exponential* term.

Thus these three Wilf classes have generating functions that are D-finite, algebraic, and (almost certainly) non-D-finite respectively.

For the 16 Wilf classes of length-5 PAPs there is only one, $Av(12345)$, for which the generating function is known [9]. It is D-finite. In one other case, $Av(31245)$, the growth constant is known [7], and for $Av(53421)$ the growth constant can be expressed in terms of that of $Av(1324)$ [8], which has been estimated to some accuracy in [11]. These three known growth constant results can all be obtained from Theorem 4.2 in [8], alternatively proved as Theorem 3.2 in [1].

We wrote a general purpose program to generate the coefficients, which is very efficient, but does have significant memory demands. It is memory, rather than time, that has limited the length of the series we can generate. There is considerable variation in both time and memory requirements for different Wilf classes. For example, for $Av(43251)$ we

obtained the series to $O(x^{26})$ in 2 hours 50 mins of CPU time, using a single core, and 212 GB of memory. By contrast, for $Av(52341)$ we obtained the series to $O(x^{23})$ in 15 hours of CPU time, using a single core, and 600 GB of memory. To obtain the next coefficient would require more than 2TB of memory. In this way, we obtained series for all Wilf classes of various lengths from $O(x^{23})$ to $O(x^{27})$.

This almost doubles the length of the available series in 14 of the 16 Wilf classes. As mentioned, $Av(12345)$ is completely solvable, so an arbitrary number of coefficients is available, and for $Av(31245)$ a special purpose program has been written giving 38 coefficients [5]. Our program is described in the next section.

In Sec. 3 we give a brief description of Stieltjes moment sequences, describing the properties that we need in this work. In Sec. 4 we give a little more detail about what is known about classical patterns of length 5, and give a table classifying all 120 permutations into the 16 Wilf classes, based on a combination of known symmetries and direct enumeration. In Sec. 5 we describe the general principles of series analysis as needed here, in Sec. 6 we discuss the ratio method, and in Sec. 7 we discuss the extension of the ideas of the previous two sections to the analysis of stretched-exponential singularities. In Sec. 8 we describe the method of differential approximants, which is what is needed in Sec. 9, where we discuss the idea of series extension. More precisely, we are able to obtain many more *approximate* coefficients than we have exact coefficients to a sufficient degree of accuracy that we can apply the previously described ratio methods and their extensions.

Using all these techniques, we analyse the 16 Wilf classes in Sec. 10. Sec. 11 comprises a brief discussion and conclusion.

One *caveat* we would like to make is that the only singularity types we are considering are pure power-law and stretched exponentials, motivated of course by the fact that these are the only singularity types we have encountered for PAPs of shorter length. And indeed, it is clear that many of the series behave in one or other of these ways. But series such as Av(12453) are not as clear cut. So if there is another singularity type, or even stretched exponentials with additional multiplicative logarithmic corrections, we are not testing for that.

2   Program to generate coefficients

We first wrote a general-purpose algorithm which produced data for all Wilf classes for patterns up to $O(x^{16})$ (which means 17 terms in the generating function). Our algorithm takes time $O(T \cdot s_n)$, where T is the time taken to check whether a pattern is avoided, and s_n is the number of PAPs of length n. Our algorithm has essentially zero memory requirements, while the testing time T is $O(n^{k-1})$ for a pattern of length k.

We then learnt of Kuszmaul's algorithm [28] which also takes time $O(T \cdot s_n)$, but T is now $O(k)$, though the trade-off is significantly greater memory requirements. However, for the permutations up to length 16 the memory requirements are still modest, and Kuszmaul's algorithm is faster than ours – typically by a factor of 10 – so we see no point in describing ours.

Inoue and Minao proposed a radically different algorithm [27], though applied to

the somewhat different problem of topological ordering, which does not examine each permutation individually. It uses a permutation set description technique called πDD which has established reasonably efficient algorithms for various set operations on such representations [26]. We describe this in the following subsection, applied to the problem of the enumeration of PAPs.

2.1 The Rot-πDD algorithm

Imagine one has variables $x_1, x_2, \ldots, x_n$.

A *Binary Decision Diagram* (BDD) [10] is an often compact method of representing sets of sets of these variables. It is a tree representation where each node is one of the variables. To determine whether a particular set $S \subseteq \{x_1, x_2, \ldots, x_n\}$ is in the represented set of sets, start at the root node, and traverse down the tree. At each node x_i it will have two children. Take the left if $x_i \notin S$ and the right if $x_i \in S$. Eventually one will reach a leaf which is 0 or 1 representing respectively that S is not or is in the represented set of sets. As a complete binary tree, there are 2^n leaves and this is not compact; however merging of isomorphic subgraphs and eliminating nodes whose children are isomorphic can often reduce the representation to a more efficient version.

Importantly, there are well known reasonably efficient algorithms for various operations on a BDD, including set intersection, union, and cardinality.

There is a slight improvement on a BDD called a *Zero Suppressed Decision Diagram* (ZDD) [29] which can be more compact by suppressing nodes whose positive edge points to the zero leaf. More precisely, the compression ratios of BDD and ZDD depend on the particular set of sets they represent. BDD was historically invented to represent a Boolean function and has a better compression ratio on Boolean functions empirically. On the other hand, ZDD can compress a set of sparse sets well empirically. Since permutation sets on combinatorial problems have some mathematical structure and tend to be represented as sparse sets of operations, we selected ZDD as the base structure of πDD rather than BDD.

A permutation can be represented as a set of operations that generate the permutation. This means that a set of permutations can be represented as a BDD or better ZDD where each variable is one of the operations that generate the permutation. This is called a *Permutation Decision Diagram* (πDD). Again the point is that the representation of the πDD may be significantly more compact than a list of the permutations it represents [30]. The set of operations that are used in the standard representation of a πDD are element exchanges. Any n element permutation can be written as the composition of up to $n-1$ two element exchanges. A Rot-πDD [27] is the same idea except that the variables are now, instead of a swap of elements i and j, a rotation of the elements between i and j inclusive. Conceptually this is a very similar approach; in practice however the constructed sets for many problems using the Rot-πDD representation is significantly more compact than the πDD representation. Details of the algorithm and examples of its use in general are given in Sec. 4.1 of [24]. Specific application to enumerating length-5 PAPs are given in Sec. 4.4 of [24]. A more succinct description of the algorithm is currently

being written, see [25]. The BDD library and also the Rot-πDD library can be found at https://github.com/Shin-ichi-Minato/SAPPOROBDD.

The publications [26] and [24] describe a method of constructing all permutations that do *not* avoid a pattern by constructing representations of permutations that include the pattern in each possible specific choice of elements in the permutation. These sets turn out to be significantly more compact with the Rot-πDD representation than the πDD representation. The union of these sets (performed with standard ZDD algorithms) is the set of all non-PAPs. Subtracting from the set of all permutations then gives the set of all PAPs.

2.2 Comparison with previous algorithms

The πDD algorithm has significantly different computational requirements to the $O(T \cdot s_n)$ algorithms which visit each pattern avoiding permutation, and can in principle be significantly faster than any such algorithm, at the cost of a higher memory consumption.

While good theoretical complexity analysis is not available for the πDD or Rot-πDD algorithms, given current computer speeds and memory capacities, the Rot-πDD algorithm is multiple orders of magnitude faster than algorithms like Kuszmaul's or our prior algorithm that inspect each pattern avoiding permutation individually, typically producing an extra 8 or 10 terms. To put this into context, previous algorithms would require years of CPU time to produce series of this length, rather than hours required by the Rot-πDD algorithm.

The data in this paper were computed using Inoue's Rot-πDD program, and the early terms were independently checked by both our early simple algorithm and Kuszmaul's program. The first 20 digits of the later terms were confirmed by the method of series extension, described below. Full details can be found in [24].

The calculations were done using the Research Computing Services facilities hosted at the University of Melbourne, more precisely the Melbourne Research Cloud, based on the OpenStack cloud computing platform. The virtual machine used had 2TB of memory and 48 cores and was running on a physical node with an AMD EPYC 7702 64-Core Processor. The algorithm varies in efficiency even within a single Wilf class. Accordingly, we experimented and determined which permutation was most efficiently enumerated within each Wilf class, and of course chose that permutation in order to find the longest possible series.

The code can be found at https://github.com/darsein.

3 Stieltjes moment sequences

The classical *Stieltjes moment problem* considers a numerical sequence $\mathbf{a} \equiv \{a_n\}$, $n \geqslant 0$ in which a_n can be expressed as the integral

$$a_n = \int_{\Gamma} x^n d\rho(x)$$

for all $n \geqslant 0$, where the support $\Gamma \subseteq \mathbb{R}$, and ρ is a measure. If the measure ρ is differentiable, then it has a *density* or *density function* $\mu(x) = \rho'(x)$. In which case the above equation becomes

$$a_n = \int_\Gamma x^n \mu(x) dx.$$

There are several equivalent conditions that the sequence $\mathbf{a}$ must satisfy in order to be a Stieltjes moment sequence, or equivalently, for such a density function to exist, which must of course be non-negative.

The Hankel matrix $H_n^\infty(\mathbf{a})$ is defined as

$$H_n^\infty(\mathbf{a}) = \begin{bmatrix} a_n & a_{n+1} & a_{n+2} & \cdots \\ a_{n+1} & a_{n+2} & a_{n+3} & \cdots \\ a_{n+2} & a_{n+3} & a_{n+4} & \cdots \\ \vdots & \vdots & \vdots & \ddots \end{bmatrix}$$

The following theorem was proved in part by Stieltjes and in part by Gantmakher and Krein. In particular, the properties (a) and (d) (below) were shown to be equivalent by Stieltjes [37], while these were later shown to be equivalent to (b) and (c) by Gantmakher and Krein[14].

Theorem 1. *For a sequence $\mathbf{a} \equiv \{a_n\}$, $n \geqslant 0$, the following are equivalent: (a) There exists a positive measure ρ on $\Gamma \in [0, \infty)$ such that*

$$a_n = \int_\Gamma x^n d\rho(x).$$

(b) The matrices $H_0^\infty(\mathbf{a})$ and $H_1^\infty(\mathbf{a})$ are both positive semidefinite.
(c) The matrix $H_0^\infty(\mathbf{a})$ is totally positive (all of its minors are non-negative).
(d) There exists a sequence of real numbers $\alpha_0, \alpha_1, \ldots \geqslant 0$ such that the generating function $A(x)$ for the sequence $a_0, a_1, \ldots$ satisfies

$$A(x) = \sum_{n=0}^\infty a_n x^n = \cfrac{\alpha_0}{1 - \cfrac{\alpha_1 x}{1 - \cfrac{\alpha_2 x}{1 - \cdots}}}$$

A sequence that satisfies the equivalent conditions of Theorem 1 is called a *Stieltjes moment sequence*.

One reason for attempting to identify combinatorial sequences as Stieltjes moment sequences is that such sequences are log-convex. To see that a Stieltjes moment sequence is log-convex, it suffices to observe that for each $n \geqslant 1$, the expression $a_{n+1}a_{n-1} - a_n^2 \geqslant 0$ is a minor of $H_0^\infty(\mathbf{a})$, so this expression is non-negative by condition (c).

Log-convexity of the sequence $\mathbf{a}$ implies that the ratios $\frac{a_n}{a_{n-1}}$ provide lower bounds to the growth constant μ of the sequence. In the case that $\mathbf{a}$ is a Stieltjes moment sequence,

we can use the above properties to compute stronger lower bounds for μ, using a method first given by Haagerup, Haagerup and Ramirez-Solano [22].

Using the coefficients $a_0, a_1, \ldots, a_n$, we calculate the terms $\alpha_0, \alpha_1, \ldots \alpha_n$ in the continued fraction representation above. It is easy to see that the coefficients of $A(x)$ are non-decreasing in each α_j. Hence $A(x)$ is (coefficient-wise) bounded below by the generating function $A_n(x)$, defined by setting $\alpha_n, \alpha_{n+1}, \alpha_{n+2}, \ldots$ to 0. Therefore, the growth rate μ_n of $A_n(x)$ is no greater than the growth rate μ of $A(x)$. The growth rates $\mu_1, \mu_2, \ldots$ clearly form a non-decreasing sequence, and, since the coefficients of $A_n(x)$ are log-convex, $\mu_n \geqslant a_n/a_{n-1}$. It follows that this sequence $\mu_1, \mu_2, \ldots$ of lower bounds converges to the exponential growth rate μ of $\mathbf{a}$.

Assuming further that the sequences $\alpha_0, \alpha_2, \alpha_4 \ldots$ and $\alpha_1, \alpha_3, \alpha_5 \ldots$ are non-decreasing, as we find empirically in all of the cases we consider, we can get stronger lower bounds for the growth rate by setting $\alpha_{n+1}, \alpha_{n+3}, \ldots$ to α_{n-1} and $\alpha_{n+2}, \alpha_{n+4}, \ldots$ to α_n. For this sequence the exponential growth rate of the corresponding sequence $\mathbf{a}$ is $b_n \equiv (\sqrt{\alpha_n} + \sqrt{\alpha_{n-1}})^2$. By the method with which we constructed this bound, it is clear that $(\sqrt{\alpha_n} + \sqrt{\alpha_{n-1}})^2 \geqslant \mu_n$. Hence, the lower bounds $(\sqrt{\alpha_n} + \sqrt{\alpha_{n-1}})^2$ converge to the growth constant μ. In all cases considered here these bounds are monotone in n, and can be numerically extrapolated. In particular, if the ratios of the original coefficients,

$$ r_n = \frac{a_n}{a_{n-1}} \sim \mu \left(1 + \frac{c}{n^\theta} + o\left(\frac{1}{n^\theta} \right) \right), $$

then we have heuristic arguments, (not yet a proof), that $b_n \sim const. \cdot n^\beta$, where $\beta = 2\theta/(2-\theta)$. This gives us the appropriate power against which to extrapolate the bounds. Also, if $\alpha_n \leqslant \alpha_{n+2}$ for each n and the limit

$$ \lim_{n \to \infty} \alpha_n $$

exists, then it is equal to $\mu/4$. We have calculated these "bounds" for all sixteen Wilf classes.

4   Classical patterns of length 5

It is known that of the 120 possible classical PAPs of length five, there are just 16 Wilf classes. Only one of these 16 cases is solved, that of $Av(12345)$, in the sense that the generating function can be explicitly written down. In eqn. (34) in [9] the solution is given as a second-order linear inhomogeneous ODE, and furthermore the generating function is shown to be a Stieltjes moment sequence. Furthermore, it is simply related to the moments of a 4-step random walk in two dimensions, as well as to the number of $2n$-step polygons on the diamond lattice.

In Tables 2 and 3 we give the coefficients to various orders from 23 to 27 for all 16 Wilf classes, as generated by our program.

We have analysed the series in order to estimate the growth constants and the associated exponent of the sub-dominant term. We also identified those cases which we believe have a

25314	41352								
31524	42513	24153	35142						
35214	41253	23514	41532	25134	43152	25413	31452		
43251	15234	13452	25431	23415	51432	41235	53214		
34215	51243	14532	23541	15423	32451	43125	52134		
53124	42135	13542	24531	15243	34251	32415	51423		
32541	14523	34125	52143						
35124	42153	24513	31542	25143	34152	41523	32514		
31245	54213	12453	35421	12534	43521	21453	35412	21534	43512
23145	54132	23154	45132	31254	45213				
42351	15324	14352	25341	24315	51342	41325	52314		
42315	51324	15342	24351						
12345	54321	45321	12354	12543	34521	21345	54312	21354	45312
21543	34512	23451	15432	32145	54123	32154	45123	43215	51234
35241	14253	13524	42531	24135	53142	31425	52413		
53241	14235	13425	52431						
53421	12435	21435	53412	13245	54231	13254	45231		
52341	14325								

Table 1: The distribution of the 120 possible length-5 pattern-avoiding permutations among the 16 Wilf classes. Note that the entries for the classes $Av(31245)$ and $Av(12345)$ are split across two lines of the table.

stretched-exponential singularity, as observed in the case of $Av(1324)$ PAPs, and discussed above.

We have also identified the permutation classes of all 120 possible length-5 classical permutations. The obvious equality

$$s_n(n_1 n_2 n_3 n_4 n_5) = s_n(n_5 n_4 n_3 n_2 n_1)$$

reduces the identification to 60 possible classes. Further reductions follow from complement and inverse operations, and the result [3]

$$s_n(543 n_4 n_5) = s_n(345 n_4 n_5),$$

the result proved in [36] that

$$s_n(354 n_4 n_5) = s_n(435 n_4 n_5),$$

the result [4] that

$$s_n(12 \cdots k\tau) = s_n(k(k-1) \cdots 1\tau),$$

where τ is a permutation of the elements $\{k+1..l\}$, and

$$s_n(\tau k k - 1) = s_n(\tau(k-1)k),$$

where now τ is a permutation of the elements $\{1, \ldots, k-2\}$, proved in [35]. Further identification of Wilf classes using the Wilf-equivalence between two-layer permutations

and monotone permutations of the same length, as discussed in [38], has also been made. The remaining equivalences were established by direct enumeration of the outstanding classes using our computer program. The results are shown in Table 1 below. Anticipating our numerical results, we have listed the 16 classes in increasing order of the (estimated) growth constants. The result of this is that they are *not* necessarily listed in increasing order of the last-known coefficient. Of course, if sufficiently many coefficients were known, these two orderings must be identical.

n	Av(25314) A256195	Av(31524) A256196	Av(35214) A256197	Av(43251) A256203
7	4578	4579	4579	4581
8	33184	33216	33218	33283
9	258757	259401	259483	260805
10	2136978	2147525	2149558	2171393
11	18478134	18632512	18672277	18994464
12	165857600	167969934	168648090	173094540
13	1535336290	1563027614	1573625606	1632480259
14	14584260700	14937175825	15093309024	15851668551
15	141603589300	146016423713	148223240022	157824649955
16	1400942032152	1455402205257	1485673163882	1605839173312
17	14087464765300	14753501614541	15159644212775	16652321922596
18	143689133196008	151783381341695	157142812302992	175596537163347
19	1484090443264936	1582029822426003	1651865171372967	1879357191026029
20	15499968503875136	16681492660789425	17582693993265148	20382942631855557
21	163501005435759505	177726496203056670	189269329080075275	223719376672365073
22	1740170514634463426	1911230701872865231	2058215511081891400	2482094083780961295
23	18671118911254798454	20726637978574528119	22589841589522026553	27808544385768051233
24	201805434191401310152	226497541235099049284	250032335770049925668	314346011323933283258
25	2195829593847519231848	2492440846906157577367	2788899325208909923567	3582440933577530273836
26	24039330044242839545400		31329479505464363566868	41134198972534449502215
27				4755817663780165253358137

n	Av(34215) A256205	Av(53124) A256199	Av(32541) A256204	Av(35124) A256198
7	4581	4580	4581	4580
8	33285	33252	33284	33249
9	260886	260202	260847	260092
10	2173374	2161837	2172454	2159381
11	19032746	18858720	19015582	18815124
12	173741467	171285237	173461305	170605392
13	1642533692	1609282391	1638327423	1599499163
14	15999488304	15561356705	15939733122	15427796984
15	159917206735	154246419725	159099927785	152487271455
16	1634681988983	1562151687940	1623799173782	1539554179950
17	17042352950764	16121960812335	16900201391546	15836801521762
18	180798150762914	169178376076607	178967276844263	165625811815111
19	1948027746498015	1801800479418116	1924689980696921	1757953168747511
20	21282786390947602	19446010522240384	20987593594256974	18908510233855411
21	235446451502773103	212394673429250090	231734179050033660	205838673911323648
22	2634317655935012208	2345064355131025130	2587835777992844938	2265393020812413370
23	29778833170013213300	26148064110299271293	29198736751160012102	25182471016157568626
24	339796984870771392635	294190661855648481179	332575357468837097628	282511039355447739772
25	3910755764784092153311	333733597067441425688	3821024002600674745994	3196265588333257586119
26	45365839293606522375359		44252507544177176282956	3644564306682928379492
27	53009860115855305094014			41860063162767027037089

Table 2: Coefficients from order 6 to 27 for the half of the 16 Wilf classes with smaller growth constant μ. The initial terms in all sequences are $1, 1, 2, 6, 24, 119, 694$. The classes are arranged in increasing order with respect to μ, reading left to right from the top row.

5   Series analysis

The method of series analysis has, for many years, been a powerful tool in the study of a variety of problems in statistical mechanics, combinatorics, fluid mechanics and computer science. In essence, the problem is the following: Given the first N coefficients of the series expansion of some function, (where N is typically as low as 5 or 6, or as high as 100,000 or more), determine the asymptotic form of the coefficients, subject to some underlying

assumption about the asymptotic form, or, equivalently, the nature of the singularity of the function.

n	Av(31245) A116485	Av(42351) A256200	Av(42315) A256206	Av(12345) A047889
7	4581	4580	4581	4582
8	33286	33252	33287	33324
9	260927	260204	260967	261808
10	2174398	2161930	2175379	2190688
11	19053058	18861307	19072271	19318688
12	174094868	171341565	174426353	178108704
13	1648198050	1610345257	1653484169	1705985883
14	16085475576	15579644765	16165513608	16891621166
15	161174636600	154541844196	162344264849	172188608886
16	1652590573612	1566713947713	1669261805697	1801013405436
17	17292601075489	16190122718865	17526017429722	19274897768196
18	184246699159418	170171678529883	187472773174466	210573149141896
19	1995064785620557	1816001425551270	2039233971499931	2343553478425816
20	21919480341617102	19646035298044543	22520066337196663	26525044132374656
21	244015986016996763	215179180467834605	252141732452056894	304856947930144656
22	2749174129340156922	2383465957654163227	2858721279079666465	3553266124166899872
23	31313478171012371344	26673704385975326866	32786666580814894741	41952101272633801376
24	360255986786421416732	301342110309622207830	380034587229949049485	501228159413699278144
25	4183070452633759090955	3434155564505269412223	4448342812221497172384	6054582181256780696704
26	48986523769015357032198	39453283522954708152659	52542550112506952504622	73884542290182291304704
27	5782066800078321677926243	4566682456064320178686247		910193895170720544149248

n	Av(35241) A256201	Av(53241) A256202	Av(53421) A256207	Av(52341) A256208
7	4580	4580	4582	4582
8	33254	33256	33325	33325
9	260285	260370	261853	261863
10	2163930	2166120	2191902	2192390
11	18900534	18945144	19344408	19358590
12	172016256	172810050	178582940	178904675
13	1621031261	1633997788	1713999264	1720317763
14	15739870457	15939893003	17019444969	17132629082
15	156855197297	159820729208	174149184184	176055309619
16	1599233708733	1641980432159	1830279810276	1861037944163
17	16638560125635	17242378256155	19703572779755	20185165186517
18	176269571712376	184674461615836	216769635980879	224150069984572
19	1898076560618372	2013829450204384	2432308876304981	2543698932578158
20	20742488003444465	22324460502429244	27788506478197951	29451619807433107
21	229747253093647567	251250502143635615	322770995262901091	347417296695040510
22	2576270755655436479	2867467023751687892	3806657237502632706	4170088041714300134
23	29218474225923168362	33152272498223444540	45532086120583546634	50874753262007210667
24	334868638387692996919	387935538721724466875	551794232925251495478	
25	3875365114838257507148	4590792008759551665335	6769119579399164598190	
26	4525635390354788096108	5490147167332777 2683658	83991144346393508063125	
27				

Table 3: Coefficients from order 6 to 27 for the half of the 16 Wilf classes with larger growth constant μ. The initial terms in all sequences are $1, 1, 2, 6, 24, 119, 694$. The classes are arranged in increasing order with respect to μ, reading left to right from the top row.

A typical example is the generating function of self-avoiding walks (SAWs) in dimension two or three. This is believed to behave as

$$F(z) = \sum_n c_n z^n \sim C \cdot (1 - z/z_c)^{-\gamma}. \tag{1}$$

In this case, among regular two-dimensional lattices, the value of z_c is only known for the hexagonal lattice [12], while $\gamma = 43/32$ is believed to be the correct exponent value for all two-dimensional lattices, but this has not been proved.

The method of series analysis is used when one or more of the critical parameters is not known. For example, for the three-dimensional versions of the above problems, none of the quantities C, z_c or γ are exactly known. From the binomial theorem it follows from (1) that

$$c_n \sim \frac{C}{\Gamma(\gamma)} \cdot z_c^{-n} \cdot n^{\gamma-1}, \tag{2}$$

where $a_n \sim b_n$ means that $\lim_{n\to\infty} a_n/b_n = 1$. Here C, z_c, and γ are referred to as the critical amplitude, the critical point (usually the radius of convergence) and the critical exponent respectively. In combinatorics one often refers to the *growth constant* μ, which is $\mu = 1/z_c$, as the coefficients are dominated by the term μ^n.

Obtaining these coefficients is typically a problem of exponential complexity, as is the case with our algorithm, described in Sec. 2. The usual consequence is that that fewer than 50 terms are known (and in some cases far fewer).

6 Ratio Method

The ratio method was perhaps the earliest systematic method of series analysis employed, and is still the most useful method when only a small number of terms are known. It is of course assumed that $\lim_{n\to\infty} a_n/a_{n-1}$ exists and is equal to the growth constant. For length-5 PAPs this has been proved by Atapour and Madras [2]. From eqn. (2), it follows that the *ratio* of successive terms

$$r_n = \frac{c_n}{c_{n-1}} = \frac{1}{z_c}\left(1 + \frac{\gamma-1}{n} + \mathrm{o}(\frac{1}{n})\right). \tag{3}$$

It is then natural to plot the successive ratios r_n against $1/n$. If the correction terms $\mathrm{o}(\frac{1}{n})$ can be ignored[1], such a plot will be linear, with gradient $\frac{\gamma-1}{z_c}$, and intercept $\mu = 1/z_c$ at $1/n = 0$.

As an example, we apply the ratio method to the solved case of $Av(12345)$ PAPs [9]. We will use 101 coefficients, to align with our analysis of other PAPs subsequently. Plotting successive ratios against $1/n$ results in the plot shown in Fig. 1. The critical point is known to be at $z_c = 1/16$.

From the figure one sees that the locus of points still displays some curvature. There are two possible explanations. One is that there is a stretched exponential term, the other is that we have a pure power law, but that the term of order $1/n^2$ has a coefficient much greater than the coefficient of the term of order $1/n$, so makes a strong contribution for small values of n. To see if this is in fact the case, we can eliminate the term of order $1/n^2$ by forming the modified ratios:

$$r2_n \equiv \frac{n^2 r_n - (n-1)^2 r_{n-1}}{2n} = \mu\left(1 + \frac{g-1}{2n} + O\left(\frac{1}{n^3}\right)\right). \tag{4}$$

We show in Fig. 2 a plot of $r2_n$ against $1/n$, which now appears to be completely linear, supporting the second explanation for the initial curvature of the ratio plot. Indeed, further numerical investigation of the ratios show that they behave as

$$r_n = \mu\left(1 - \frac{7.5}{2n} + \frac{131.25}{n^2} + O\left(\frac{1}{n^3}\right)\right),$$

showing the very large $\mathrm{O}(1/n^2)$ term compared to the order $1/n$ term.

---

[1]For a purely algebraic singularity eqn. (1), with no confluent terms, the correction term will be $\mathrm{O}(\frac{1}{n^2})$.
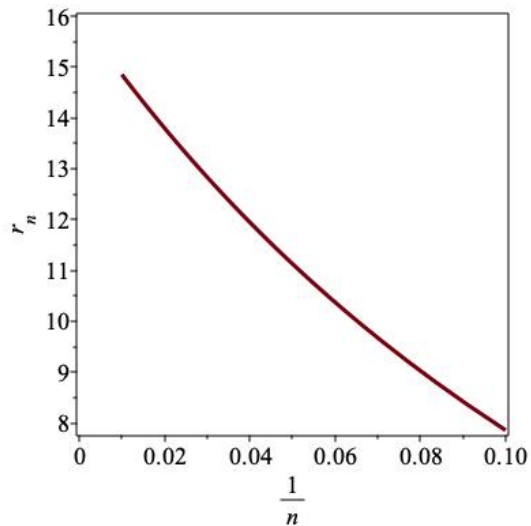
Figure 1: Plot of ratios against $1/n$ for $Av(12345)$ PAPs. A straight line through the last few data points intercepts the ratios axis at $\mu = 1/z_c$.
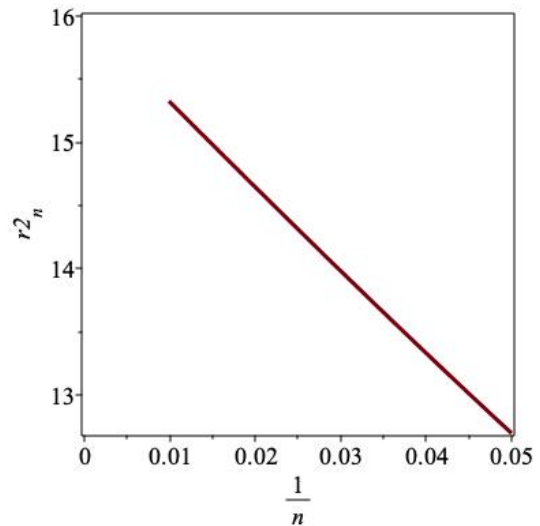
Figure 2: Plot of modified ratios $r2_n$ against $1/n$ for $Av(12345)$ PAPs, showing linearity.
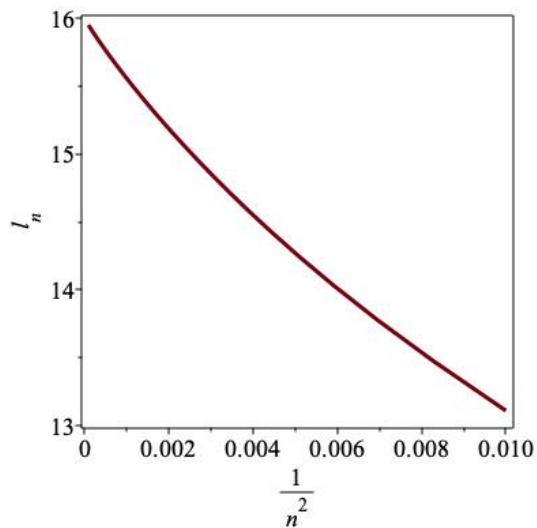
Figure 3: Plot of linear intercepts l_n against $1/n^2$ for $Av(12345)$ PAPs. A straight line through the last few data points intercepts the vertical axis at $\mu = 1/z_c$.
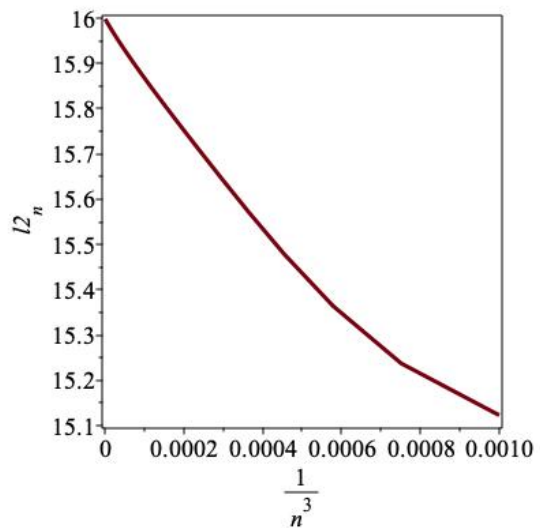

Figure 4: Plot of quadratic intercepts $l2_n$ against $1/n^3$ for $Av(12345)$ PAPs. A straight line through the last few data points intercepts the vertical axis at $\mu = 1/z_c$.

Visual extrapolation to $1/z_c \approx 16$ is quite obvious. A straight line drawn through the last $4 - 6$ data points intercepts the horizontal axis around $1/n \approx 0.07$. Thus the
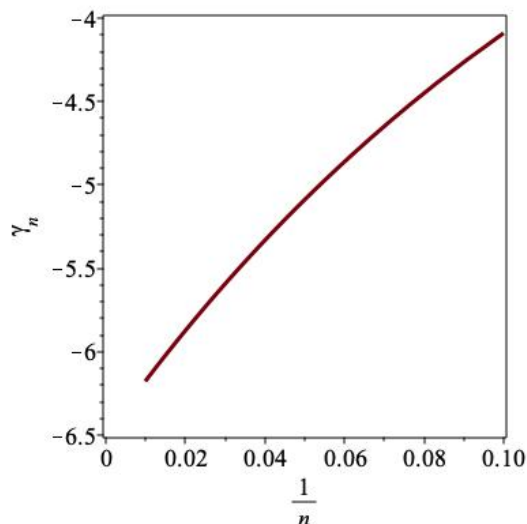
Figure 5: Plot of exponent estimates γ_n against $1/n$ for $Av(12345)$ PAPs, assuming $\mu = 16$. Visual extrapolation suggests $\gamma \approx -6.5$.
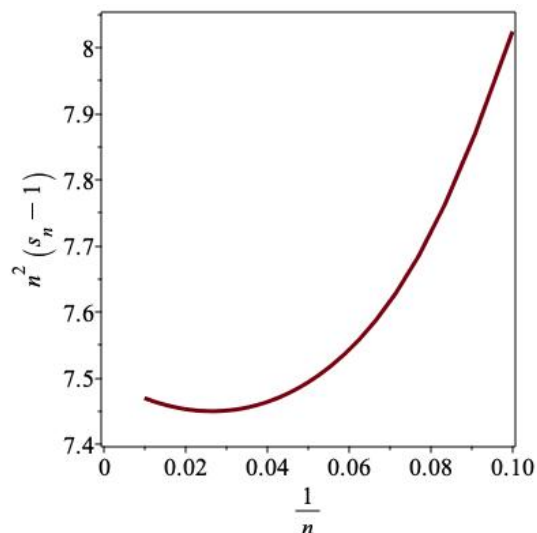
Figure 6: Plot of $n^2(s_n - 1)$ against $1/n$ for $Av(12345)$ PAPs, which should go to $-g = 7.5$ as $n \to \infty$.

gradient is approximately $\frac{16-7.8}{-0.07} \approx -117$, from which we conclude that the exponent $\gamma - 1 \approx -117 \cdot z_c \approx -7.3$. It is known that the exact value is $\gamma - 1 = -7.5$, which is in approximate agreement with this simple graphical analysis.

Linear intercepts l_n eliminate the $O\left(\frac{1}{n}\right)$ term in eqn. (3), so in the case of a pure power-law singularity, one has

$$l_n \equiv nr_n - (n-1)r_{n-1} = \mu\left(1 + \frac{c}{n^2} + O\left(\frac{1}{n^3}\right)\right).$$

The linear intercepts in this case are shown in Fig. 3, and it is clear that they are converging to the known limit $\mu = 16$ rather more rapidly than are the plain ratios. In the case of a pure power-law, where sub-dominant terms in the ratios decrease by successive factors of $1/n$, this process can be continued. For example, we can eliminate terms of order $1/n^2$ by forming quadratic estimators

$$l2_n \equiv \frac{n^2 l_n - (n-1)^2 l_{n-1}}{2l - 1} = \mu\left(1 + \frac{c}{n^3} + O\left(\frac{1}{n^4}\right)\right).$$

The quadratic intercepts are shown in Fig. 4, and it is clear that they are converging to the known limit $\mu = 16$ even more rapidly than are the linear intercepts or ratios.

Various refinements of the method can be readily derived. If the critical point is known exactly, it follows from eqn. (3) that estimators of the exponent γ are given by

$$\gamma_n = n(z_c \cdot r_n - 1) + 1 = \gamma + o(1).$$

The estimators γ_n are shown in Fig. 5, and it can be seen that they are plausibly going to a limit, as $1/n \to 0$, of -6.5, which is the exact value of the exponent in this case.

If the critical point is not known exactly, one can still estimate the exponent γ. From eqn. (3) it follows that

$$\delta_n = 1 + n^2 \left(1 - \frac{r_n}{r_{n-1}} \right) = \gamma + o(1). \tag{5}$$

The estimators δ_n are shown in Fig. 7, and it can be seen that they too are plausibly going to a limit, as $1/n \to 0$, of $\gamma = -6.5$.
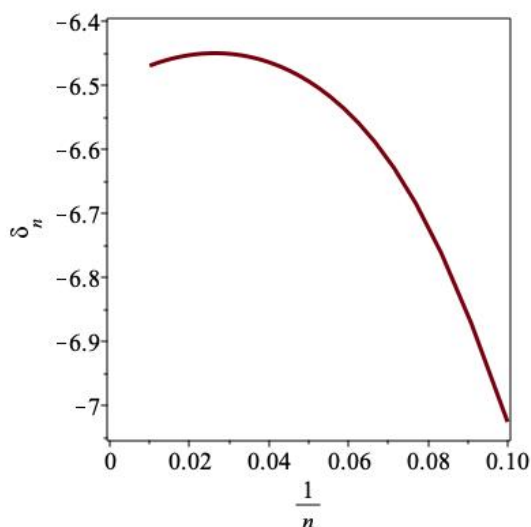
Figure 7: Plot of exponent estimates δ_n against $1/n$ for $Av(12345)$ PAPs.
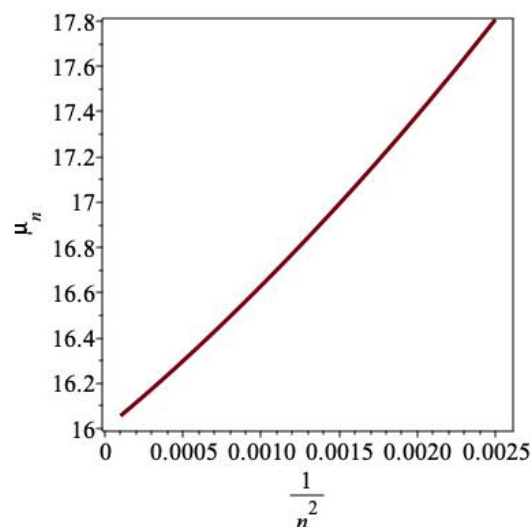
Figure 8: Plot of growth-constant estimates μ_n against $1/n^2$ for $Av(12345)$ PAPs.

Similarly, if the exponent γ is known, estimators of the growth constant μ are given by

$$\mu_n = \frac{nr_n}{n + \gamma - 1} = \mu + o(1/n).$$

The estimators μ_n are shown in Fig. 8, and it can be seen that they are very plausibly going to a limit, as $1/n \to 0$, of $\mu = 16$.

The explanation of Fig. 6 is given in Section 7.1 after eqn. (13). The figure provides compelling evidence for a pure power-law singularity in this case.

7   Functions with non-power-law singularities

A number of solved, and, we believe, unsolved problems that arise in lattice critical phenomena and algebraic combinatorics have coefficients with a more complex asymptotic form, with a sub-dominant term that varies as $\mu_1^{n^\sigma}$ as well as a power-law term varying as

n^g. Perhaps the best-known example of this sort of behaviour is the number of partitions of the integers – though in that case the leading exponential growth term μ^n is absent (or equivalently $\mu = 1$). The form of the coefficients c_n in the general case is

$$c_n \sim C \cdot \mu^n \cdot \mu_1^{n^\sigma} \cdot n^g. \tag{6}$$

An example from combinatorics is given by Dyck paths enumerated not just by length, but also by height (defined to be the maximum vertical distance of the path from the horizontal axis). Let $d_{n,h}$ be the number of Dyck paths of length $2n$ and height h. The OGF is then[2]

$$D(x, y) = \sum_{n,h} d_{n,h} x^{2n} y^h, \text{ and } [x^{2n}]D(x, y) = \sum_{h=1}^{n} d_{n,h} y^h. \tag{7}$$

For $y < 1$ let $A = 2^{5/3}\pi^{5/6}/\sqrt{3}$, $E = 3\left(\frac{\pi}{2}\right)^{2/3}$ and $r = -\log y$. Then one finds that $[x^{2n}]D(x, y)$ is given by eqn. (6) with $C = \frac{1-y}{y^2}r^{1/3}A$, $\mu = 4$, $\mu_1 = \exp(-Er^{2/3})$, $\sigma = 1/3$, and $g = -5/6$.

Note however that such singular behaviour *can* arise from D-finite ODEs as the asymptotic form of the coefficients of some generating function at an *irregular* singular point. However, as shown by Garrabrant and Pak [15], if a counting sequence is integer-valued, grows at most exponentially, and is D-finite, then such singular behaviour cannot occur. From this it follows that all PAPs exhibiting stretched-exponential behaviour cannot be D-finite. Of course, in no case have we proved the existence of stretched-exponential behaviour, so the asserted non-D-finiteness is also conjectural.

Applying the ratio method to such singularities requires some significant changes. These were first developed in [18], where further details and more examples can be found. In the next subsection we give a summary, including as much detail as is needed for our analysis.

7.1 Ratio method for stretched-exponential singularities

If

$$b_n \sim C \cdot \mu^n \cdot \mu_1^{n^\sigma} \cdot n^g, \tag{8}$$

then the ratio of successive coefficients $r_n = b_n/b_{n-1}$, is

$$r_n = \mu \left(1 + \frac{\sigma \log \mu_1}{n^{1-\sigma}} + \frac{g}{n} + \frac{\sigma^2 \log^2 \mu_1}{2n^{2-2\sigma}} + \frac{(\sigma - \sigma^2)\log \mu_1 + 2g\sigma \log \mu_1}{2n^{2-\sigma}} \right. $$
$$\left. + \frac{\sigma^3 \log^3 \mu_1}{6n^{3-3\sigma}} + \mathrm{O}(n^{2\sigma-3}) + \mathrm{O}(n^{-2}) \right). \tag{9}$$

---

[2]One of us (AJG) posed this problem at an Oberwolfach meeting in March 2014. Within 24 hours Brendan McKay produced this solution. See also [32].

It is usually the case that σ takes the simple values $1/2$, $1/3$, $1/4$ etc.[3].

When $\sigma = \frac{1}{2}$, (9) specialises to

$$r_n = \mu \left(1 + \frac{\log \mu_1}{2\sqrt{n}} + \frac{g + \frac{1}{8}\log^2 \mu_1}{n} + \frac{\log^3 \mu_1 + (6 + 24g)\log \mu_1}{48 n^{3/2}} + \mathrm{O}(n^{-2}) \right), \qquad (10)$$

and when $\sigma = \frac{1}{3}$, to

$$r_n = \mu \left(1 + \frac{\log \mu_1}{3 n^{2/3}} + \frac{g}{n} + \frac{\log^2 \mu_1}{18 n^{4/3}} + \frac{(2 + 6g)\log \mu_1}{18 n^{5/3}} + \mathrm{O}(n^{-2}) \right), \qquad (11)$$

and when $\sigma = \frac{1}{4}$, to

$$r_n = \mu \left(1 + \frac{\log \mu_1}{4 n^{3/4}} + \frac{g}{n} + \frac{\log^2 \mu_1}{32 n^{3/2}} + \frac{(3 + 8g)\log \mu_1}{32 n^{7/4}} + \mathrm{O}(n^{-2}) \right). \qquad (12)$$

The presence of the term $\mathrm{O}(\frac{1}{n^{1-\sigma}})$ in the expression for the ratios above means that a ratio plot against $1/n$ will display curvature, which can be usually be removed by plotting the ratios against $1/n^{1-\sigma}$, with $\sigma = 1/2$ or $1/3$, or $1/4$ etc. A full study of such a situation applied to $Av(1324)$ PAPs can be found in [11].

Of course as we saw in the previous section, curvature in the ratio plots can also arise from a pure power-law singularity if the coefficient of the term $\mathrm{O}(\frac{1}{n^2})$ in the expression for the ratio is much greater than the coefficient of the term $\mathrm{O}(\frac{1}{n})$. This situation can be identified by plotting the modified ratios, as defined by eqn. (4). If these are linear, that is strong evidence of a pure power-law singularity.

One can also apply the following test to identify those situations when we have a stretched-exponential singularity. From eqn. (9), we note that, with $s_n = r_n/r_{n-1}$,

$$n^2(s_n - 1) = (\sigma - 1) \cdot \sigma \log \mu_1 \cdot n^\sigma - g. \qquad (13)$$

(If $\sigma = 1/2$, g must be replaced by $g - \log \mu_1^2/8$.) With a stretched-exponential term, this sequence should diverge with n. In the presence of a pure power-law, the sequence should tend to $-g$ as $n \to \infty$. We show in Fig. 6 that in this case the sequence is indeed tending to $-g = 7.5$ as expected.

Unfortunately the observation that a ratio plot against $1/n^{1-\sigma}$ will linearise the plot does not provide a sufficiently precise method to estimate the value of σ. One can usually distinguish between, say, $\sigma = 1/2$ and $\sigma = 1/3$ in this way, but one cannot be much more precise than that. However, as we now show, one can extend the ratio method to provide direct estimates for the value of σ.

From (9), one sees that

$$(r_n/\mu - 1) = \sigma \log \mu_1 \cdot n^{\sigma - 1} + O\left(\frac{1}{n}\right). \qquad (14)$$

---

[3]In statistical mechanical models, the value of the exponent σ is simply related to the fractal dimension d_f of the object through $\sigma = 1/(1 + d_f)$.

Accordingly, a plot of $\log(r_n/\mu - 1)$ versus $\log n$ should be linear, with gradient $\sigma - 1$. We would expect an estimate of σ close to that which linearised the ratio plot.

This log-log plot will usually be visually linear, but the local gradients are changing slowly as n increases. It is therefore worthwhile extrapolating the local gradients. To do this, from (14), we form the estimators

$$\tilde{\sigma}_n = 1 + \frac{\log|r_n/\mu - 1| - \log|r_{n-1}/\mu - 1|}{\log n - \log(n-1)}. \tag{15}$$

This can be extrapolated against $1/n^\sigma$, using any approximate value of σ.

A second estimator of σ follows from eqn. (8). Define

$$c_n \equiv \log(b_n/\mu^n) \sim \log C + \log \mu_1 \cdot n^\sigma + g \cdot \log n,$$

then setting

$$d_n \equiv c_n - c_{n-1} \sim \sigma \log \mu_1 \cdot n^{\sigma-1} + g/n, \tag{16}$$

a log-log plot of d_n against n should be linear with gradient $\sigma - 1$. Note that if σ is closer to zero than to 1, there is likely to be some competition between the two terms in the expansion.

This way of estimating σ requires knowledge of, or at worst a very precise estimate of, the growth constant μ. While μ is exactly known in some cases, more generally μ is not known, and must be estimated, along with all the other critical parameters. In order to estimate σ without knowing μ, we can use one (or both) of the following estimators:

From eqn. (9), it follows that

$$r_{\sigma_n} \equiv \frac{r_n}{r_{n-1}} \sim 1 + \frac{(\sigma - 1)\log \mu_1}{n^{2-\sigma}} + \mathrm{O}(1/n^2), \tag{17}$$

so σ can be estimated from a plot of $\log(r_{\sigma_n} - 1)$ against $\log n$, which should have gradient $\sigma - 2$. Again, the local gradients can be calculated and plotted against $1/n^\sigma$, using any approximate value of σ.

Another estimator of σ when μ is not known follows from eqn. (8),

$$a_{\sigma_n} \equiv \frac{b_n^{1/n}}{b_{n-1}^{1/(n-1)}} \sim 1 + \frac{(\sigma - 1)\log \mu_1}{n^{2-\sigma}} + \mathrm{O}(1/n^2), \tag{18}$$

so again σ can be estimated from a plot of $\log(a_{\sigma_n} - 1)$ against $\log n$. Again, estimates of σ are found by extrapolating the local gradient against $1/n^\sigma$.

While these two estimators are equal to leading order, they differ in their higher-order terms. Which of the two is more informative seems to vary from problem to problem. However, we generally use both.

From eqn. (9), if we know (or conjecture) μ and σ, we can use this to estimate μ_1, as

$$\left(\frac{r_n}{\mu} - 1\right) \cdot n^{1-\sigma} \sim \sigma \cdot \log(\mu_1). \tag{19}$$

7.2 Direct fitting

Another, perhaps obvious, idea is to try and fit the critical parameters directly to the assumed asymptotic form,
$$b_n \sim C \cdot \mu^n \cdot n^g$$
in the case of a pure power law singularity, or

$$b_n \sim C \cdot \mu^n \cdot \mu_1^{n^\sigma} \cdot n^g$$

in the case of a stretched exponential singularity.

For a stretched exponential singularity,

$$\log b_n \sim \log C + n \log \mu + n^\sigma \log \mu_1 + g \log n. \tag{20}$$

So if σ is known, or assumed, there are four unknowns in this linear equation. It is then straightforward to solve the linear system

$$\log b_k = c_1 k + c_2 k^\sigma + c_3 \log k + c_4 \tag{21}$$

for $k = n-2$, $n-1$, n, $n+1$ with n ranging from 3 to $N-1$, where N is the highest known power of the series. We refer to this as a *4-point fit*. Then c_1 estimates $\log(\mu)$, c_2 estimates $\log(\mu_1)$, c_3 estimates g and c_4 gives estimators of $\log C$. An obvious variation arises in those cases where, say, μ is known. Then one can solve

$$\log(b_k) - k \log \mu = c_1 k^\sigma + c_2 \log k + c_3 \tag{22}$$

from three successive coefficients, as before increasing the order of the lowest coefficient used by one until one runs out of coefficients. We refer to this as a *3-point fit*.

Alternatively, one can fit the *ratios* to

$$r_n = c_1 + \frac{c_2}{n^{1-\sigma}} + \frac{c_3}{n} + \frac{c_4}{n^{2-2\sigma}}, \tag{23}$$

from four successive coefficients, as before increasing the order of the lowest coefficient used by one until one runs out of coefficients. Then c_1 estimates μ, c_2 estimates $\mu \cdot \sigma \log(\mu_1)$, c_3 estimates $\mu \cdot g$ (or $\mu(g - \log^2(\mu_1)/8)$ if $\sigma = 1/2$), and c_4 gives estimators of $\mu \cdot \sigma^2 \log^2(\mu_1)/2$.

If the value of both μ and σ are known, one can fit three parameters to

$$r_n - \mu = \frac{c_1}{n^{1-\sigma}} + \frac{c_2}{n} + \frac{c_3}{n^{2-2\sigma}}, \tag{24}$$

where c_1 estimates $\mu \cdot \sigma \log \mu_1$ c_2 estimates $\mu \cdot g$ and c_3 estimates $\mu \cdot \sigma^2 \log^2(\mu_1)/2$.

For the case of a pure power law singularity, we find the idea of direct fitting most useful to estimate the amplitude C when the exponent g is known or conjectured. In that case one can estimate μ and C by fitting to

$$\log b_k - g \log n \sim c_1 n + c_2 + c_3/n, \tag{25}$$

where c_1 gives estimators of $\log \mu$ and c_2 gives estimators of $\log C$.

We will apply a number of these techniques in our analysis, below, of the 16 Wilf classes of length-5 PAPS.

8 Differential approximants

The generating functions of some problems in enumerative combinatorics are sometimes algebraic, such as that for $Av(1342)$ PAPs, sometimes D-finite, such as $Av(12345)$ PAPs, sometimes differentially algebraic, and sometimes transcendentally transcendental. The not infrequent occurrence of D-finite solutions was the origin of the method of *differential approximants*, a very successful method of series analysis for power-law singularities [17].

The basic idea is to approximate a generating function $F(z)$ by solutions of differential equations with polynomial coefficients. That is to say, by D-finite ODEs. The singular behaviour of such ODEs is well documented (see e.g. [13, 23]), and the singular points and exponents are readily calculated from the ODE.

The key point for series analysis is that even if *globally* the function is not describable by a solution of such a linear ODE (as is frequently the case) one expects that *locally,* in the vicinity of the (physical) critical points, the generating function is still well-approximated by a solution of a linear ODE, when the singularity is a generic power law (1).

An Mth-order differential approximant (DA) to a function $F(z)$ is formed by matching the coefficients in the polynomials $Q_k(z)$ and $P(z)$ of degree N_k and L, respectively, so that the formal solution of the Mth-order inhomogeneous ordinary differential equation

$$\sum_{k=0}^{M} Q_k(z)(z\frac{\mathrm{d}}{\mathrm{d}z})^k \tilde{F}(z) = P(z) \tag{26}$$

agrees with the first $N = L + \sum_k (N_k + 1)$ series coefficients of $F(z)$.

Constructing such ODEs only involves solving systems of linear equations. The function $\tilde{F}(z)$ thus agrees with the power series expansion of the (generally unknown) function $F(z)$ up to the first N series expansion coefficients. We normalise the DA by setting $Q_M(0) = 1$, thus leaving us with N rather than $N+1$ unknown coefficients to find. The choice of the differential operator $z\frac{\mathrm{d}}{\mathrm{d}z}$ in (26) forces the origin to be a regular singular point. The reason for this choice is that most lattice models with holonomic solutions, for example, the free-energy of the two-dimensional Ising model, possess this property. However this is not an essential choice.

From the theory of ODEs, the singularities of $\tilde{F}(z)$ are approximated by zeros z_i, $i = 1, \ldots, N_M$ of $Q_M(z)$, and the associated critical exponents γ_i are estimated from the indicial equation. If there is only a single root at z_i this is just

$$\gamma_i = M - 1 - \frac{Q_{M-1}(z_i)}{z_i Q_M'(z_i)}. \tag{27}$$

Estimates of the critical amplitude C are rather more difficult to make, involving the integration of the differential approximant. For that reason the simple ratio method approach to estimating critical amplitudes is often used, whenever possible taking into account higher-order asymptotic terms [20].

Details as to which approximants should be used and how the estimates from many approximants are averaged to give a single estimate are given in [20]. Examples of the

application of the method can be found in [18]. In that work, and in this, we reject so-called *defective* approximants, typically those that have a spurious singularity closer to the origin than the radius of convergence as estimated from the bulk of the approximants. Another method sometimes used is to reject outlying approximants, as judged from a histogram of the location of the critical point (i.e. the radius of convergence) given by the DAs. It is usually the case that such distributions are bell-shaped and rather symmetrical, so rejecting approximants beyond two or three standard deviations is a fairly natural thing to do.

9 Coefficient prediction

In [19] we showed that the ratio method and the method of differential approximants work serendipitously together in many cases, even when one has stretched exponential behaviour, in which case neither method works particularly well in unmodified form.

To be more precise, the method of differential approximants (DAs) produces ODEs which, by construction, have solutions whose series expansions agree term by term with the known coefficients used in their construction. Clearly, such ODEs implicitly define *all* coefficients in the generating function, but if N terms are used in the construction of the ODE, all terms of order z^N and beyond will be approximate, unless the exact ODE is discovered, in which case the problem is solved, without recourse to approximate methods.

What we have found is that it is useful to construct a number of DAs that use all available coefficients, and then use these to predict subsequent coefficients. Not surprisingly, if this is done for a large number of approximants, it is found that the predicted coefficients of the term of order z^n, where $n > N$, agree for the first $k(n)$ digits, where k is a decreasing function of n. We take as the predicted coefficients the mean of those produced by the various DAs, with outliers excluded, and as a measure of accuracy we take the number of digits for which the predicted coefficients agree, or the standard deviation. These two measures of uncertainty are usually in good agreement.

Now it makes no logical sense to use the approximate coefficients as input to the method of differential approximants, as we have used the DAs to obtain these coefficients. However there is no logical objection to using the (*approximate*) predicted coefficients as input to the ratio method. Indeed, as the ratio method, in its most primitive form, looks at a graphical plot of the ratios, an accuracy of 1 part in 10^4 or 10^5 is sufficient, as errors of this magnitude are graphically unobservable.

Recall that, in the ratio method one looks at *ratios* of successive coefficients. We find that the ratios of the approximate coefficients are predicted with even greater precision than the coefficients themselves by the method of DAs. That is to say, while a particular coefficient and its successor might be predicted with an accuracy of 1 part in 10^p for some value of p, the *ratio* of these successive coefficients is frequently predicted with significantly greater accuracy (the precision being typically improved by a factor varying between 2 and 20).

The DAs use all the information in the coefficients, and are sensitive to even quite small errors in the coefficients. As an example, in a recent study of some self-avoiding walk

series, an error was detected in the eighteenth significant digit in a new coefficient, as the DAs were much better converged without the last, new, coefficient[4]. The DAs also require high numerical precision in their calculation. In favourable circumstances, they can give remarkably precise estimates of critical points and critical exponents, by which we mean up to or even beyond 20 significant digits in some cases. Surprisingly perhaps, this can be the case even when the underlying ODE is not D-finite. Of course, the singularity must be of the assumed power-law form.

Predicted ratios	Actual ratios
10.463935493	10.46393544
10.654655347	10.65465504
10.828226522	10.82822539
10.986854456	10.98685140
11.132386843	11.13238007
11.266382111	11.26636895
11.390163118	11.39013998
11.504857930	11.50482182
11.611441483	11.61138359
11.710743155	11.71066190
11.803496856	11.80338255
11.890333733	11.89017822
11.971808520	11.97160282
12.048402545	12.04814337
12.120553112	12.12022972
12.188650126	12.18824275
12.252994715	12.25252103
12.313939194	12.31336663
12.371707700	12.37104982
12.426619450	12.42581319
12.478784843	12.47787509
12.528486946	12.52743256

Table 4: Ratios r_{18} to r_{39} actual and predicted from the coefficients of $Av(12453)$.

Ratio methods, and direct fitting methods, by contrast are much more robust. The sort of small error that affects the convergence of DAs would not affect the behaviour of the ratios, or their extrapolants, and would thus be invisible to them. As a consequence, approximate coefficients are just as good as the correct coefficients in such applications, provided they are accurate enough. We re-emphasise that, in the generic situation (1),

---

[4]Given 69 terms of the square-lattice self-avoiding walk series, the 70th term is predicted by 4th order ODEs to be $4190893020903935057 \times 10^{12}$. The actual coefficient is $4190893020903935054619120005916$, which differs in the nineteenth digit. An error in the eighteenth digit was thus discovered during development. Several other less dramatic examples are known where lower-order errors have been discovered by this means.

ratio type methods will rarely give the level of precision in estimating critical parameters that DAs can give. By contrast, the behaviour of ratios can more clearly reveal features of the asymptotics, such as the fact that a singularity is not of power-law type. This is revealed, for example, by curvature of the ratio plots [18].

We take, as an example, the OGF for $Av(12453)$ PAPs (see OEIS [33] A116485). This is known to order x^{38}. We will only take the coefficients to order x^{16} and use the method of series extension described above to predict the next 22 ratios, as we can compare them to the exact ratios. The results, based on 3rd order differential approximants, are shown in Table 4. For the first predicted ratio, r_{18}, the discrepancy is in the 10th significant digit. For the last predicted ratio, r_{39}, the error is in the 5th significant digit. This level of precision is perfectly adequate for ratio analysis.

In practice we find that the more exact terms we know, the greater is the number of predicted terms, or ratios that can be predicted. In this study, we typically have 26 or so series terms for each Wilf class. These are usually sufficient to predict about 100 additional ratios to 6-digit accuracy. For the singular class $Av(12453)$ we know 39 terms. In that case we are able to predict 400 further ratios.

In this study, we have extended the ratios of the generating functions of the 15 unknown Wilf classes by typically 100 additional ratios, and have analysed the resulting series by ratio methods.

10   The permutations

We have divided the 16 Wilf classes into two sets: those six which we believe have simple power-law asymptotic behaviour, so that $s_n \sim C \cdot \mu^n \cdot n^g$, and those ten that we believe have stretched-exponential behaviour similar to that exhibited by $Av(1324)$, so that the coefficients behave asymptotically as $s_n \sim C \cdot \mu^n \cdot \mu_1^{n^\sigma} \cdot n^g$, where $\sigma = 1/2$, $1/3$ or $\sigma = 1/4$.

We will go through the first examples of each in some detail, to show clearly what is involved in the analysis. Most of the other cases flow similarly *mutatis mutandis*, so we give less detail in those cases, except when some distinctive feature warrants further discussion.

Our results are summarised in Tables 5 and 6 below.

Pattern	Growth constant μ.	Lower bound, l-c.	Lower bound St.	Exponent g.	Amplitude C.
25314	12.5670 ± 0.0003	10.8809	12.4622	-3.214 ± 0.006	0.0164 ± 0.0001
31524	12.7344 ± 0.0003	11.0042	12.6417	-2.905 ± 0.01	0.00274 ± 0.00005
35214	13.275 ± 0.005	11.2336	13.1159	-3.75 ± 0.10	0.0145 ± 0.0015
43251	13.703 ± 0.001	11.4821	13.5111	-4.43 ± 0.02	$0.207 \pm 0.005.$
34215	13.945 ± 0.008	11.6002	13.7131	-4.67 ± 0.01	0.375 ± 0.08
12345	16.0	14.8735	15.9395	-7.5	275.6

Table 5: Summary of the analysis of the 6 Wilf classes of length-5 PAPs conjectured to have power-law singularities, ranked by increasing estimates of the growth constant. Lower bound l-c comes from the assumption of log-convexity. Lower bound St. comes from the stronger assumption that the series is a Stieltjes series.

Pattern	Growth constant μ.	Lower bound, l-c.	Lower bound St.	Growth constant μ_1.	Exponent σ.	Exponent g.	Amplitude C.
53124	14.24 ± 0.05	11.3441	13.5836	–	0.25 ± 0.1	–	–
32541	14.32 ± 0.04	11.5813	13.8447	–	0.27 ± 0.07	–	–
35124	14.54 ± 0.03	11.4025	13.7433	–	$1/4$	–	–
31245	$9 + 4\sqrt{2} = 14.6568\dots$	12.5274	14.3792	0.27 ± 0.02	$1/3$	-4.7 ± 0.3	–
42351	15.10 ± 0.05	11.5749	14.0314	0.0012 ± 0.0006	$1/3$	-1.25 ± 0.25	1.5 ± 0.5
42315	15.40 ± 0.04	11.8117	14.5633	0.0001 ± 0.00005	$1/4$	–	90 ± 16
35241	16.20 ± 0.04	11.6779	14.6253	0.00009 ± 0.00004	$1/3$	–	18 ± 9
53241	18.66 ± 0.05	11.9590	15.4445	0.027 ± 0.006	$1/2$	-4 ± 1	–
53421	19.4092 ± 0.0003	12.4079	16.3053	0.044 ± 0.002	$1/2$	-4.0 ± 0.5	7.4 ± 2.0
52341	24.7 ± 0.3	12.1992	17.2302	0.0015	$1/2$	–	–

Table 6: Summary of the analysis of the 10 Wilf classes of length-5 PAPs conmjectured to have stretched-exponential singularities, ranked by increasing estimates of the growth constant. Lower bound l-c comes from the assumption of log-convexity. Lower bound St. comes from the stronger assumption that the series is a Stieltjes series.

10.1 Wilf classes with pure power-law behaviour

10.1.1 Av(12345)

This case is completely solved, [9], and the generating function is D-finite. Regev [34] gave an expression for the asymptotics,

$$s_n(12345) \sim C \cdot 16^n / n^{15/2},$$

where $C = 3 \cdot 2^9 / \pi^{3/2}$. Given the existence of the known solution, it may be thought that there is little point in conducting an analysis. However, it is worthwhile as it shows the strengths and limitations of our methods, admittedly for a special, and possibly benign, case.

So, to be in accord with our knowledge of most of the other series, we assume that coefficients are known only to order x^{25}, and use these to predict the next 75 ratios. These are increasingly inaccurate with increasing order, but are still useful to the quoted order. In Fig. 9 we show the base-10 logarithm of the difference between the predicted ratios r_k^{est} and the true ratios r_k. It can be seen that this difference increases from about $10^{-16.5}$ to 10^{-9} as we move from the first predicted ratio to the 75th. (In fact, for several of the other series we use 100 predicted ratios, and in a few cases 200).

Next we carry out an extended ratio analysis. In Fig. 10 we show the predicted ratios plotted against $1/n$. There is some low order curvature, but the plot is becoming increasingly linear as n increases. The plot is going towards an intercept at $1/n = 0$ around 16.

Following Occam's razor, we assume pure power-law behaviour unless we find evidence to the contrary. For a pure power-law, we expect the linear intercepts

$$l_n = n \cdot r_n - (n-1) \cdot r_{n-1}$$

to approach the same limit more closely. As can be readily seen from eqn. (3), the linear intercepts eliminate the term $O(1/n)$ in the ratios, and in the presence of a pure power-law should vary as $O(1/n^2)$.

This process can be iterated, and the terms of order $O(1/n^2)$ eliminated by forming the quadratic intercepts

$$l2_n = \frac{n^2 \cdot l_n - (n-1)^2 \cdot l_{n-1}}{2n - 1},$$

and the cubic intercepts

$$l3_n = \frac{n^3 \cdot l2_n - (n-1)^3 \cdot l2_{n-1}}{3n^2 - 3n + 1}.$$

The linear and quadratic and cubic intercepts are shown in figs. 11, 12 and 13 respectively. It can be seen that these are approaching 16.0 more and more precisely[5]. We feel confident in estimating $\mu = 16.000 \pm 0.005$ on the basis of this study.
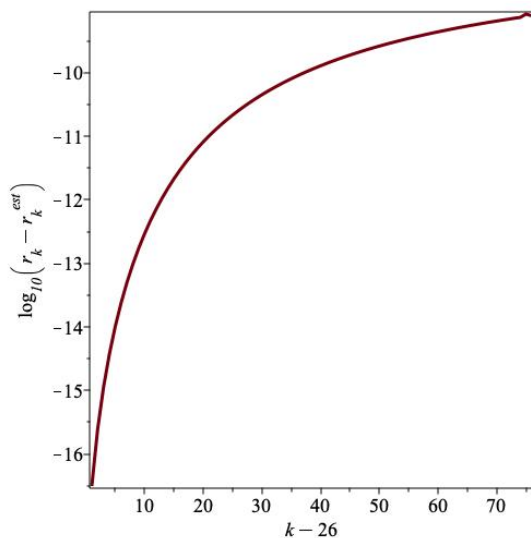
Figure 9: $\log_{10}$ of the difference between the predicted and actual ratios vs. k.
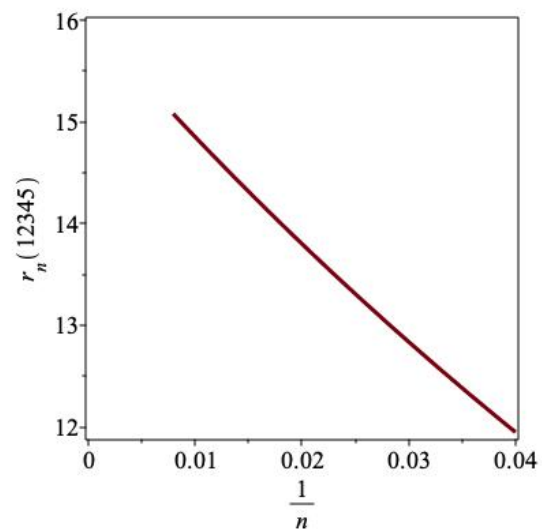
Figure 10: Ratios of $Av(12345)$ vs. $1/n$.

Using this estimate of μ, we can estimate the exponent of the sub-dominant term n^g. From the expression for the ratios (3), we have that estimators of the exponent g are given by

$$g_n = n(r_n/\mu - 1) + O(1/n).$$

These are shown in Fig. 14, and are plausibly approaching a limit $g \approx -7.5$. As we did with the ratios, these too can be linearly extrapolated by forming the estimates

$$g2_n = n \cdot g_n - (n-1) \cdot g_{n-1}.$$

These are shown in Fig. 15, and are seen to be very convincingly approaching $g = -7.5$.

---

[5]There is a small amount of "jitter" in the last few estimates of $l3_n$, reflecting the error in the (approximate) ratio estimates which gets amplified as one takes higher and higher order differences.
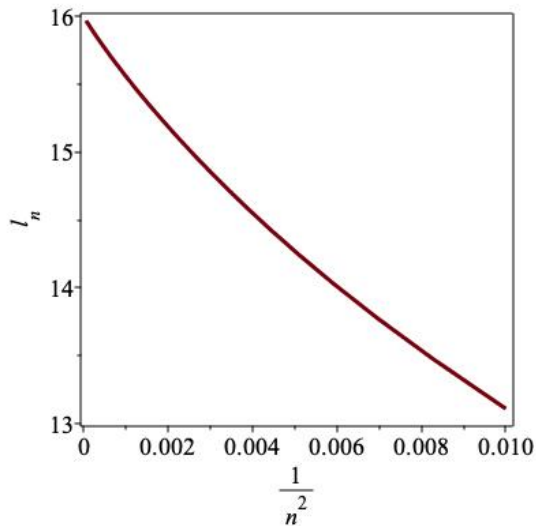
Figure 11: Linear intercepts l_n vs. $1/n^2$.
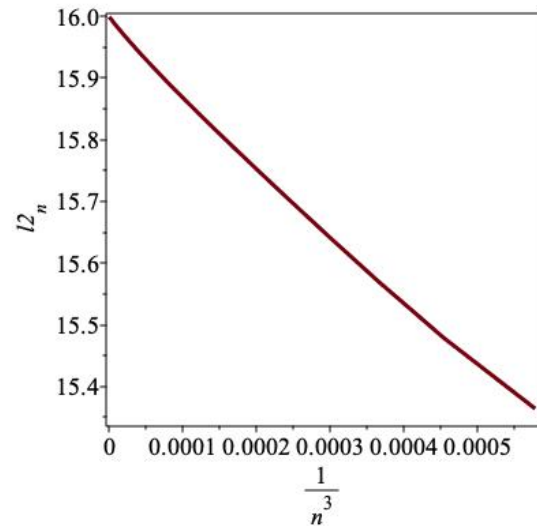
Figure 12: Quadratic intercepts $l2_n$ vs. $1/n^3$.
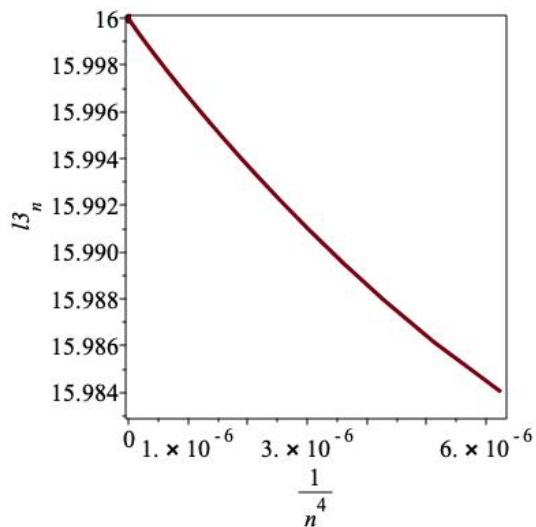
Figure 13: Cubic intercepts $l3_n$ vs. $1/n^4$.
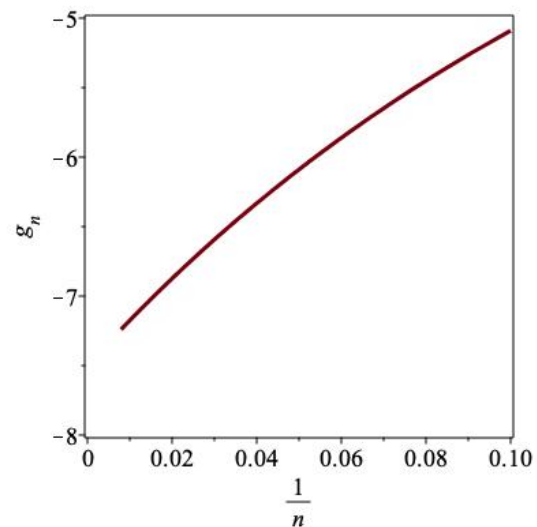
Figure 14: Estimate of exponent g, (assuming μ) vs. $1/n$.

If μ is not known, one can still estimate g from the estimators

$$g_n = n^2(1 - r_n/r_{n-1}) + O(1/n).$$

These estimators are shown in Fig. 16, and are also plausibly approaching a limit of -7.5. The maximum around $n = 35$ illustrates the great value of having additional, approximate terms. Without them, one may conclude that the plot was heading toward -7.4 or -7.3.

Of course, one can have power-law behaviour without the ratios behaving as $r_n =$
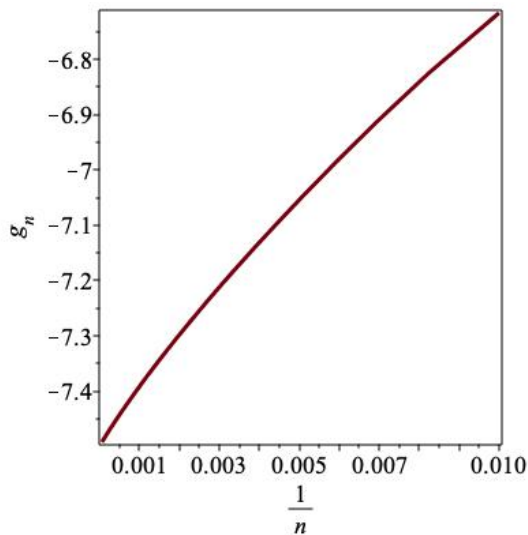
Figure 15: linear extrapolants of exponent g, (assuming μ) vs. $1/n^2$.
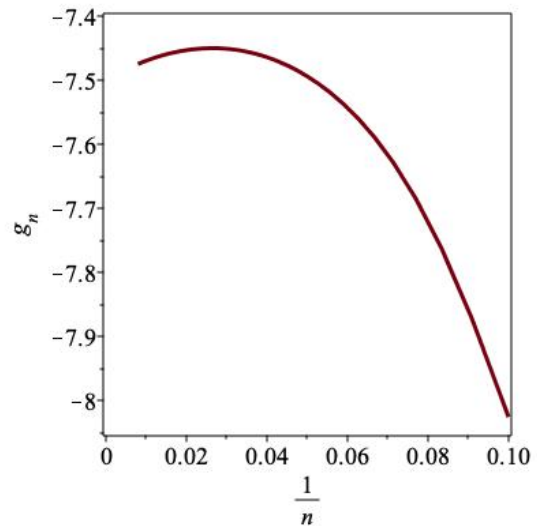
Figure 16: Estimate of exponent g vs. $1/n$ without assuming μ.

$\sum_{k=0}^{\infty} \alpha_k/n^k$ as tacitly assumed in the above analysis. For example, one might have

$$r_n \sim \mu \left(1 + g/n + h/n^{1+\Delta} + j/n^2 + \cdots\right), \tag{28}$$

where $0 < \Delta < 1$.

In the case $Av(12345)$ considered here, we know that we have pure power-law behaviour. Assuming that we do not know, one can try and estimate the value of the exponent Δ. If one has pure power-law behaviour, one should find $\Delta = 1$. This of course is a necessary, but not sufficient, condition. One might have the more unusual, but by no means impossible behaviour of the ratios

$$r_n \sim \mu \left(1 + g/n + h/n^2 + j/n^{2+\Delta} + \cdots\right).$$

We can only investigate the simpler case with any hope of success. We do this by observing from eqn. (28) that

$$\left(\frac{r_n}{\mu} - 1\right) n - g \sim \frac{h}{n^\Delta},$$

so that a log-log plot of the l.h.s. against n should have gradient $-\Delta$. In Fig. 17 we show the local gradient of the log-log plot, plotted against $1/n$, which is plausibly going to a limit $\Delta = 1$. This is consistent with the known pure power-law behaviour.

Another way of analysing the series is to fit the expression for the ratios to the available data and solve the resulting system of linear equations, as discussed in Sec. 7.2. Here we will fit the ratios to the assumed form

$$r_n = \mu \left(1 + \frac{g}{n} + \frac{h}{n^2} + \frac{j}{n^3}\right), \tag{29}$$
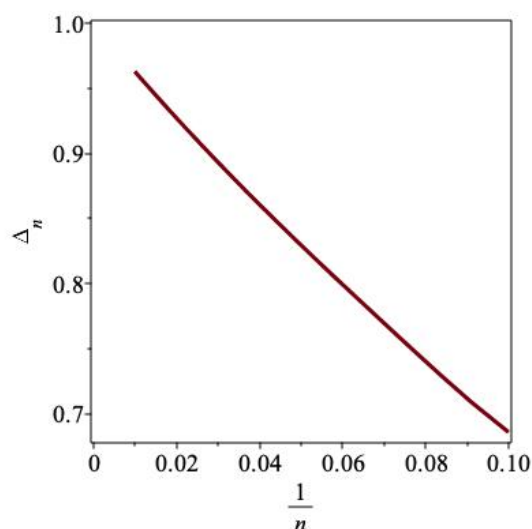
Figure 17: Estimate of exponent Δ vs. $1/n$.
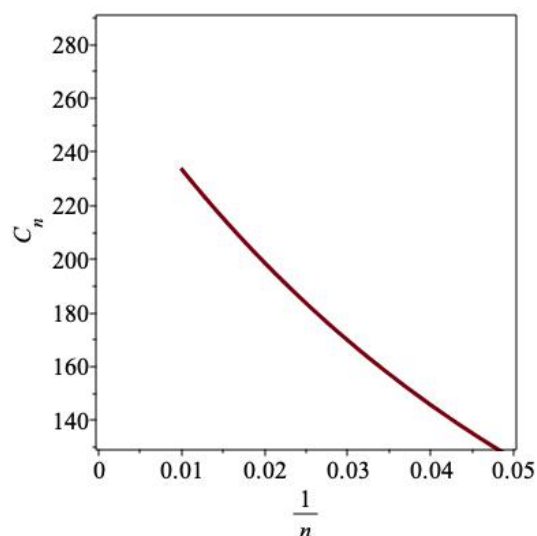
Figure 18: Estimate of amplitude C vs. $1/n$.

using successive quadruplets of ratios $r_{k-2}, r_{k-1}, r_k, r_{k+1}$, with k increasing until we run out of known ratios, to give estimates of the parameters μ, g, h, and j.

The results of this fitting are shown in the four figures figs. 19, 20, 21, 22. From the first figure, one would feel confident estimating μ at 16.0. exactly. Similarly, from the second figure, the estimate $\mu \cdot g \approx -120$ looks quite compelling, from which we conclude $g \approx -7.5$, as before. From the next two figures we estimate $\mu \cdot h \approx 540$, and $\mu \cdot j \approx -2100$, so that $h \approx 33.75$, and $j \approx 131.25$.

If we insert these parameters into eqn. (29), one predicts $r_{100} = 14.8519$. The correct value is $14.851999203\ldots$, so this asymptotic form, based on only 25 known coefficients, is pleasingly accurate.

To emphasise what has been achieved here, we took just 26 coefficients, predicted 75 further ratios using differential approximants, fitted these 100 ratios to the assumed asymptotic form, (having already produced good numerical evidence for the overall structure), and derived an asymptotic expression for the ratios which is accurate to 6 significant digits at order 100.

Finally, we can estimate the amplitude C in the expression for the asymptotic form of the coefficients, $s_n \sim C \cdot 16^n/n^{7.5}$ by forming simple estimators of C defined by

$$C_n \equiv s_n \cdot n^{7.5}/16^n.$$

These are shown Fig. 18, plotted against $1/n$ and are going to a limit around $C \approx 275$. This numerical estimate could be refined, but is known exactly (see OEIS A047889) as $C = 3 \cdot 2^9/\pi^{3/2} = 275.8458\ldots$.

Alternatively, if we knew, or conjectured, the exponent $g = -7.5$, we could use direct fitting, as described in eqn. (25) to estimate C (and indeed μ). We did this and obtained
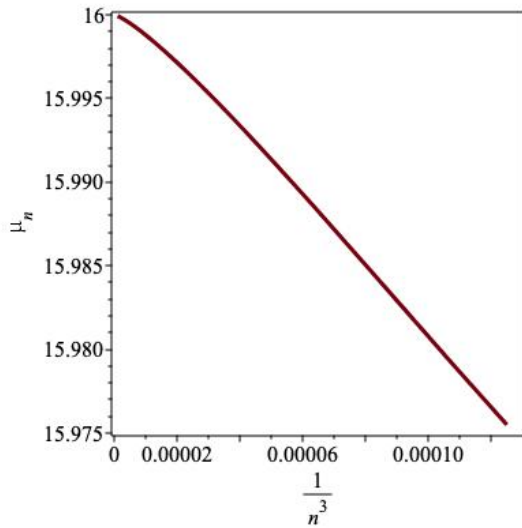
Figure 19: Estimates of μ vs. $1/n^3$.
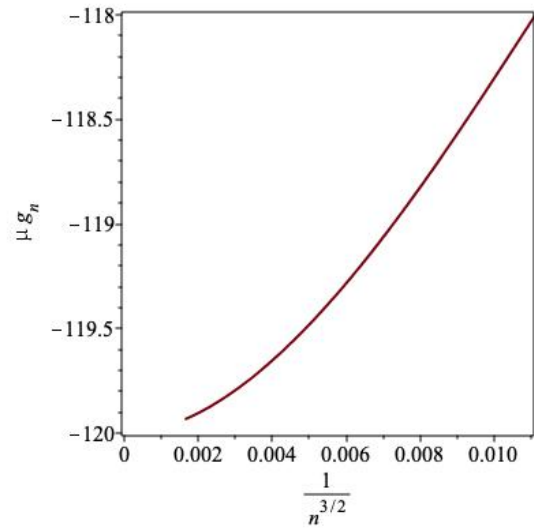
Figure 20: Estimates of $\mu \cdot g$ vs. $1/n^{3/2}$.
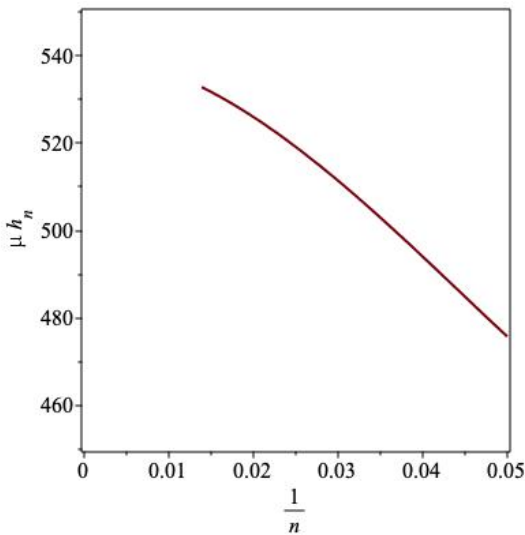
Figure 21: Estimates of $\mu \cdot h$ vs. $1/n$.
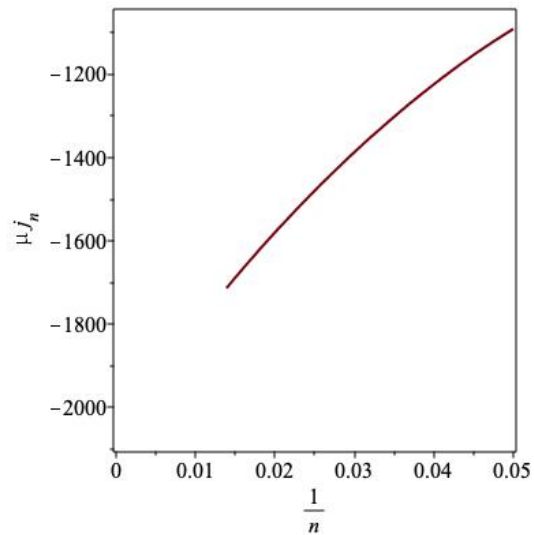
Figure 22: Estimates of $\mu \cdot j$ vs. $1/n$.

the estimates $\mu \approx 16.0000$ and $C \approx 275.6$. These are of course in complete agreement with the estimates obtained from the ratios.

If we didn't know the exact result, we would conclude that $\mu = 16.000 \pm 0.005$, $g = -7.5 \pm 0.2$, and $C \approx 275.6$. That is to say

$$s_n(12345) \sim C\mu^n \cdot n^g.$$

Of course, we know that the central estimates of μ and g are exact, and that $C = 3 \cdot 2^9/\pi^{3/2} = 275.8458\ldots$.

10.1.2 Lower bounds

It is provably the case [9] that all possible Hankel determinants constructed from the coefficients of $Av(12345)$ are positive, and monotonically increasing with the size of the matrix. As the coefficients of $Av(12345)$ therefore form a Stieltjes moment sequence, log-convexity of the coefficients follows, as discussed above, and so the ratios provide an increasing sequence of lower bounds. This gives the bound $\mu(12345) \geqslant 14.8735$ from the first 100 coefficients.

If one constructs the continued fraction representation from the exact coefficients, (see Theorem 1 above), then the terms $\alpha_0, \ldots, \alpha_{100}$ defined in Theorem 1 can be used to construct stronger bounds $(\sqrt{\alpha_n} + \sqrt{\alpha_{n-1}})^2$. Using the first 100 exact coefficients, we find the strong lower bound $\mu(25314) \geqslant 15.9395$.

The sequence of lower bounds can also be extrapolated against $1/n^2$, shown in Fig. 23, and results in an estimate of μ consistent with, but less precise than, that obtained by the direct analysis of the original, extended series.
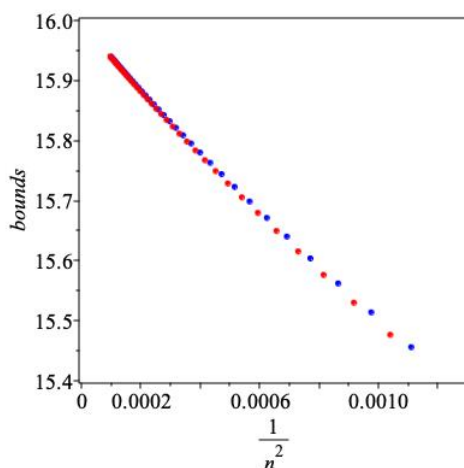
Figure 23: Stieltjes bounds vs. $1/n^2$ for $Av(12345)$.

We constructed all possible Hankel determinants from all the known (actual) coefficients for the remaining 15 unsolved Wilf classes, and observed that they too are all positive, and monotonically increasing with the size of the matrix, leading us to the conjecture that they too form a Stieltjes moment sequence. We will assume this in the analysis of the remaining 15 Wilf classes, and so provide (conjectured) lower bounds, repeating the above analysis *mutatis mutandis*.

The analysis of the remaining five Wilf classes with power-law singularities follows along similar lines, and is given in Appendix A.

10.2 Wilf classes with stretched-exponential behaviour

As discussed above in Sec. 7.1, the (naive) hallmark of such asymptotic behaviour is non-linearity – more precisely curvature – in the ratio plots. However, as seen in the

discussion of the PAP $Av(12345)$, a power-law singularity can have a ratio plot exhibiting curvature if the magnitude of the coefficient of the term $O(1/n^2)$ is significantly greater than that of the term $O(1/n)$. In that case, we formed quadratic intercepts to eliminate the $O(1/n^2)$ term, and the linearity of the ratio plot, expected for a power-law singularity, became clear.

In the case of stretched exponential singularities, the ratios behave as

$$r_n = \mu \left(1 + \frac{\sigma \log \mu_1}{n^{1-\sigma}} + \frac{g}{n} + \frac{\sigma^2 \log^2 \mu_1}{2n^{2-2\sigma}} + \frac{(\sigma - \sigma^2) \log \mu_1 + 2g\sigma \log \mu_1}{2n^{2-\sigma}} \right.$$
$$\left. + \frac{\sigma^3 \log^3 \mu_1}{6n^{3-3\sigma}} + O(n^{2\sigma-3}) + O(n^{-2}) \right). \quad (30)$$

Any ratio plot will manifest competition between the term of order $O(\frac{1}{n^{1-\sigma}})$ and that of order $O(\frac{1}{n})$. We can eliminate the latter term by constructing the linear intercepts

$$l_n \equiv n \cdot r_n - (n-1) \cdot r_{n-1} \sim \mu \left(1 + \frac{\sigma(\sigma-1) \log \mu_1}{n^{1-\sigma}} + O\left(n^{2\sigma-2}\right) + O\left(n^{\sigma-2}\right) \right.$$
$$\left. + O\left(n^{3\sigma-3}\right) + O(n^{2\sigma-3}) + O(n^{-2}) \right). \quad (31)$$

Then one can eliminate the term of order $O(1/n^2)$ by forming the quadratic intercepts

$$l2_n \equiv \frac{n^2 \cdot l_n - (n-1)^2 \cdot l_{n-1}}{2n-1} \sim \mu \left(1 + \frac{\sigma^2(\sigma-1) \log \mu_1}{2n^{1-\sigma}} + O\left(n^{2\sigma-2}\right) \right.$$
$$\left. + O\left(n^{\sigma-2}\right) + O\left(n^{3\sigma-3}\right) + O(n^{2\sigma-3}) \right). \quad (32)$$

So these quadratic intercepts eliminate both the $O(1/n)$ and the $O(1/n^2)$ terms. Plotting $l2_n$ against $1/n^{1-\sigma}$ should give a linear plot at the correct value of σ. We find this to be a more reliable indicator of the (approximate) value of the exponent σ than the simpler criterion of linearity of the ratios.

10.3 Av(12453)

This series is known up to, and including, terms of order x^{38}, given in the OEIS as sequence A116485. It is exceptional in two respects. Firstly in that so many coefficients are known, due to Biers-Ariel, who showed [5] that this pattern has properties that allowed him to write a particularly efficient algorithm for its enumeration.

Secondly, the growth constant is known exactly [7], as $\mu = 9 + 4\sqrt{2} = 14.65685\ldots$.

With this longer series we have been able to extend the ratio sequence, and coefficient sequence by 400 further terms. For maximum precision, we only use the first 200 terms in the subsequent analysis. The ratio plot, showing the ratios plotted against $1/n$ is shown in Fig. 24, and exhibits convex (w.r.t. the x-axis) curvature, which is not disappearing as n increases, unlike the situation arising for pure power-law singularities. Plotting the

modified ratios $r2_n$, defined in eqn. (4), also fails to linearise the ratio plot. This is strong evidence for a stretched-exponential singularity.

However, when the ratios are plotted against $n^{-\theta}$, where θ is in the range $(0.75 - -0.85)$ the plot is visually linear, and appears to extrapolate to the known value of μ. However, when we plot the quadratic intercepts, as defined in eqn. (32), which eliminate the effects of the $O(1/n)$ and $O(1/n^2)$ terms in the ratios, the plot is actually linearised when plotted against $n^{-\theta}$ with $\theta \approx 2/3$, as shown in Fig. 25.
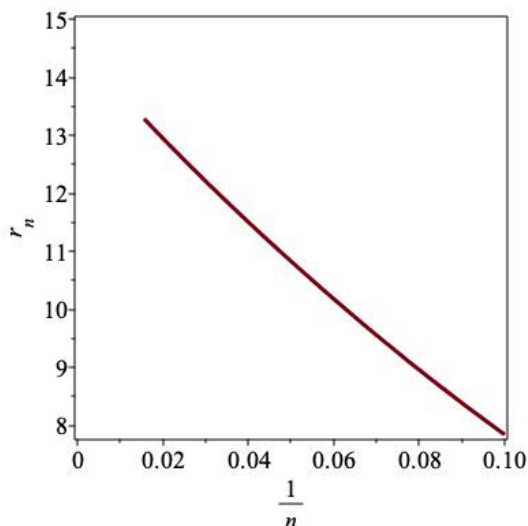
Figure 24: Ratios of $Av(12453)$ vs. $1/n$.
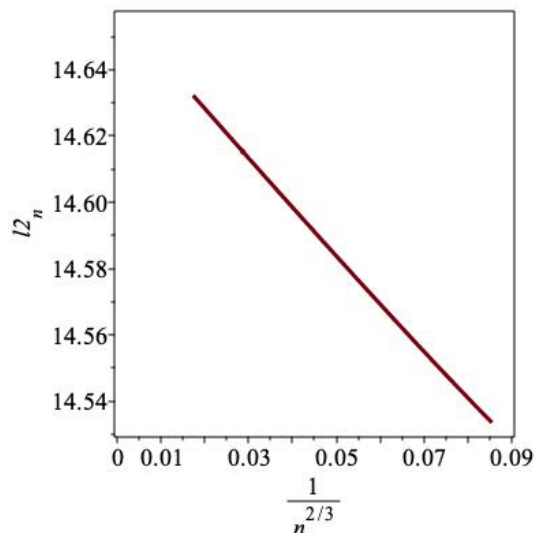
Figure 25: Quadratic intercepts of ratios vs. $1/n^{2/3}$.

To better estimate σ, we consider two ways of doing so, assuming μ is known, as it is. From eqn. (14), one sees that a plot of $\log(r_n/\mu - 1)$ versus $\log n$ should be linear, with gradient $\sigma - 1$. So we estimate σ from the gradient of this log-log plot. We would expect an estimate of σ close to that which linearised the quadratic intercepts plot. As terms of order $O(1/n)$ affect the linearity of the ratio plots, they will also have a similar effect here. So to eliminate that effect, we instead plot $\log(l_n/\mu - 1)$ versus $\log n$.

A second estimator of σ follows from eqn. (16), so that a plot of $\log(d_n)$ against $\log n$ should be linear, again with gradient $\sigma - 1$.

Both estimators will usually provide visually linear log-log plots, but the local gradients are changing as n increases. One must extrapolate the local gradients. To do this we form the estimators (in the first case)

$$\tilde{\sigma}_n - 1 = \frac{\log|l_n/\mu - 1| - \log|l_{n-1}/\mu - 1|}{\log n - \log(n-1)}. \tag{33}$$

This can be extrapolated against $1/n$. The result of doing this is shown in Fig. 26, upper curve, as $1/n$ approaches zero. The local gradient of the second estimator, given by eqn. (16), can be similarly extrapolated, and similarly plotted against $1/n$. The result of doing so is shown in Fig. 26, lower curve.

It can be seen that the second estimator displays considerable curvature, and is difficult to extrapolate, beyond saying that $\sigma > 0.15$, but the first estimator, which we expect to be more believable as it eliminates the effect of the $\mathrm{O}(1/n)$ term and the $\mathrm{O}(1/n^2)$ term in the ratios, is plausibly going to $\sigma \approx 1/3$.

An estimator of σ formed without knowledge of the growth constant μ follows from eqn. (17), so that a plot of $\log(r_{\sigma_n} - 1)$ against $\log n$, should have gradient $\sigma - 2$. However, for the same reasons as above, a more reliable estimator should follow by replacing r_n by l_n in eqn. (17), and this results in the top curve in 27.

Another estimator of σ when μ is not known is given in eqn. (18), so $\sigma - 2$ can be estimated from a plot of $\log(a_{\sigma_n} - 1)$ against $\log n$.

Again, estimates of σ are found by extrapolating the local gradient against $1/n^\sigma$. The result of doing this is shown in Fig. 27, (lower curve).

These estimates are, unsurprisingly, less precise than the estimates formed knowing μ. Indeed, the second estimator is seemingly going to a value inconsistent with the other estimators, which are consistent with our previous estimate $\sigma \approx 1/3$. We ascribe this to the strong effect of the $\mathrm{O}(1/n)$ and $\mathrm{O}(1/n^2)$ term in the ratios for this pattern.

If we accept $\sigma = 1/3$ as the most likely exact value, we can estimate the sub-dominant growth constant μ_1. From eqn. (14) it follows that

$$\left(\frac{r_n}{\mu} - 1 \right) n^{1-\sigma} \sim \sigma \cdot \log \mu_1 + \frac{g}{n^\sigma},$$

and we show in Fig. 28 a plot of the l.h.s. against $1/n^{1/3}$. From this curve, we estimate $\sigma \cdot \log \mu_1 \approx -0.45$, so $\mu_1 \approx 0.26$.

An alternative, and more precise estimate of the value of μ_1 can be made as follows: Knowing the value of μ, and assuming $\sigma = 1/3$, one can fit the remaining parameters, to the expression for the ratios, as described in eqn. (24). We show the results of this in figs. 30 and 31.

The first parameter, which we estimate to be -6.2 ± 0.2 gives $\mu \cdot \sigma \log \mu_1$. Therefore $\mu_1 = 0.28 \pm 0.01$, in quite good agreement with the less-precise estimate 0.26 given above.

The second parameter, which we estimate to be -68.5 ± 1.5 gives $\mu \cdot g$. Therefore $g = -4.67 \pm 0.1$. The third parameter, not shown, is harder to estimate, but gives us no further information, as the only unknown involved is $\log \mu_1$, which we have already estimated from the first parameter.

Alternatively, one can fit to the expression for the logarithm of the coefficients, as given in eqn. (22), and doing this we find $\log \mu_1 \approx -1.25$ and $g \approx -4.7$. So $\mu_1 \approx 0.27$. With this degree of variation in the estimates of μ_1 and g, it is not possible to reliably estimate the amplitude C.

We therefore conclude that $s_n(12453) \sim C \cdot \mu^n \cdot \mu_1^{n^\sigma} \cdot n^g$, with $\mu = 9 + 4\sqrt{2} = 14.65685\ldots$, $\sigma \approx 1/3$, $\mu_1 = 0.27 \pm 0.02$, and $g = -4.7 \pm 0.3$. We give no estimate of the amplitude C.

These parameter values explain some of the difficulties we encountered in this analysis. The ratios behave as

$$r_n \sim \mu \left(1 - \frac{0.44}{n^{2/3}} - \frac{4.7}{n} + \cdots \right).$$

One sees that the coefficient of the $O(n^{-2/3})$ term is about $1/10$ of that of the $O(1/n)$ term, which explains why we had to eliminate the $O(1/n)$ and $O(1/n^2)$ terms to be able to focus on those terms that arose from the stretched-exponential. That said, we still find the presence of a stretched-exponential term for this pattern mildly surprising, as several other PAPs which clearly exhibit stretched-exponential behaviour (42315, 35241, 53241, 53421, 52341) are all "superclasses" of 1324, while this pattern is a "super-pattern" of 1243, which has a power-law singularity.
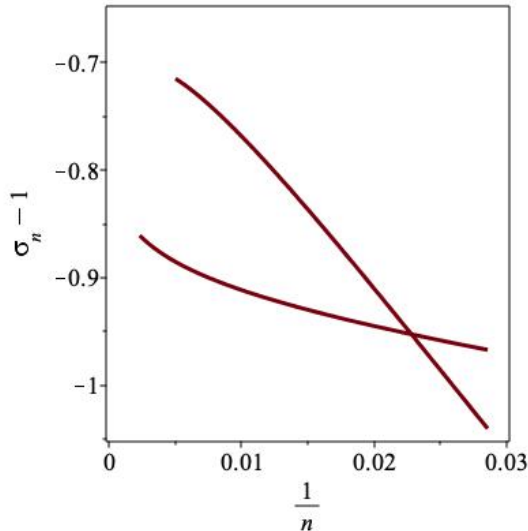
Figure 26: Estimate of exponent $\sigma - 1$ vs. $1/n$. First method, upper curve (as $1/n \to 0$), second method, lower curve.
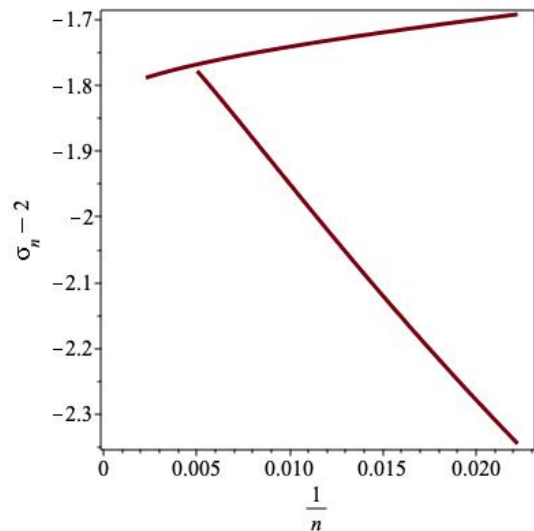
Figure 27: Estimate of exponent $\sigma - 2$ vs. $1/n$ without knowing μ. First method, upper curve, second method, lower curve.

10.3.1 Lower bounds

While there is little point in obtaining bounds in this case where the growth constant is exactly known, it is perhaps of interest to see how close the bounds are to the exact value. Assuming that the coefficients form a Stieltjes moment sequence, the consequent log-convexity gives the bound $\mu(12453) \geqslant 12.5274$. If the 400 predicted coefficients are believed, this improves the bound to $\mu(12453) \geqslant 14.4008$. From the continued-fraction representation, we obtain the lower bound 14.3792. In Fig. 32 we show these Stieltjes bounds plotted against the appropriate power of n. It can be seen they are extrapolating to the top-leftmost corner of the plot, which corresponds to μ.

The analysis of the remaining nine Wilf classes with stretched-exponential singularities follows along similar lines, and is given in Appendix B.
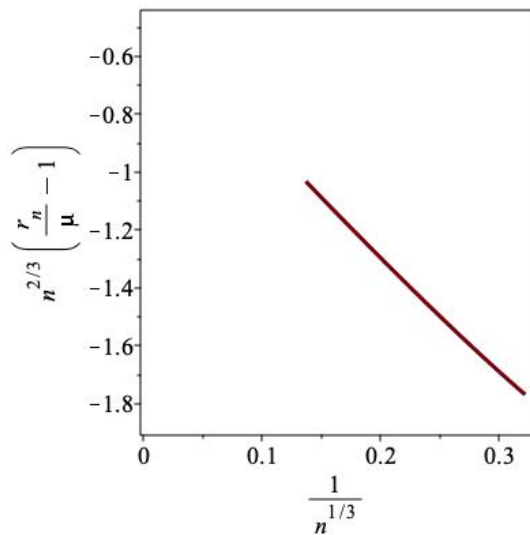
Figure 28: Estimate of μ_1 vs. $1/n^{1/3}$.
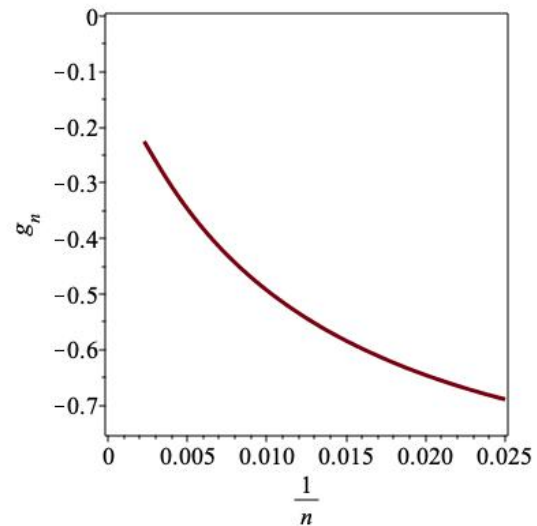
Figure 29: Estimators of exponent g vs. $1/n$ for $Av(12453)$.
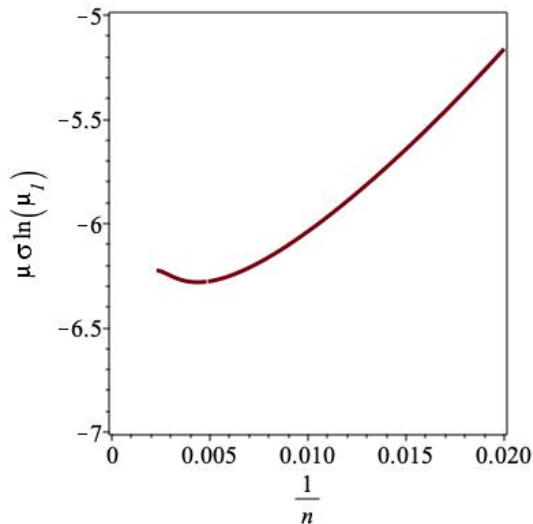
Figure 30: Estimate of $\mu \cdot \sigma \log \mu_1$ vs. $1/n$.
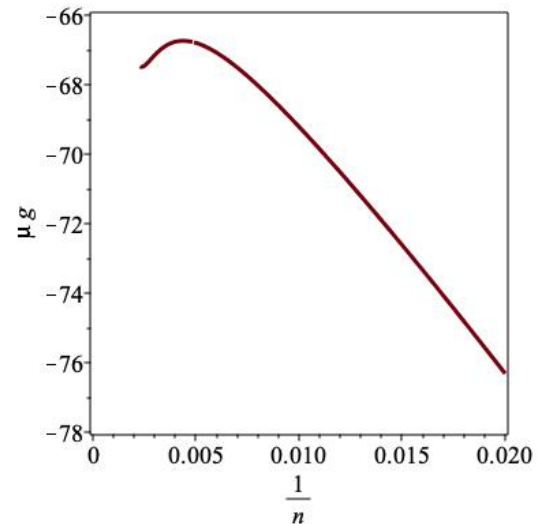
Figure 31: Estimators of exponent $\mu \cdot g$ vs. $1/n$.

11 Conclusion

This is the first of a series of papers we propose, analysing the sixteen length-5 classical pattern-avoiding permutations. The analysis given here is based on series expansions. We are also developing new Monte Carlo algorithms to provide further information, such as the shape of a typical permutation, as well as providing an alternative route to investigating the growth constants.
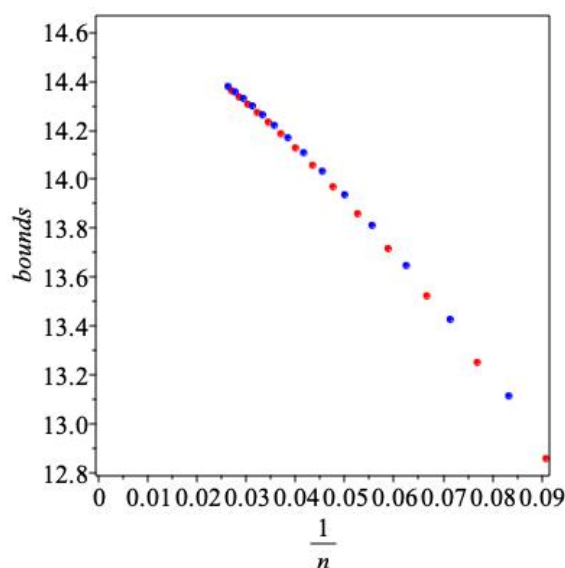
Figure 32: Stieltjes bounds vs. $1/n$ for $Av(12453)$.

Here we have extended the number of known coefficients for fourteen of the sixteen classes, see table 2 and 3. Using sequence extension and a variety of methods of series analysis we have estimated the growth constant of all classes, and have estimate the sub-dominant power-law term associated with the exponential growth, or the stretched-exponential exponent. Repeating the *caveat* made in the introduction, the only singularity types we are considering here are pure power-law and stretched exponentials, motivated of course by the fact that these are the only singularity types we have encountered for PAPs of shorter length. However, if there is another singularity type, or even stretched exponentials with additional logarithms terms, we are not testing for that.

In six of the sixteen classes cases we found the familiar power-law behaviour, so that the coefficients behave like $s_n \sim C\mu^n n^g$, while in the remaining ten cases we find a stretched exponential as the sub-dominant term, so that the coefficients behave like $s_n \sim C\mu^n \mu_1^{n^\sigma} n^g$, where $0 < \sigma < 1$.

We have also classified the 120 possible permutations into the 16 distinct classes, see table 1. While the existence of 16 Wilf classes has been known for some time, the classification of all 120 possible permutations into these 16 classes has not previously been made explicit, as far as we know.

We give lower bounds to the growth constant in all cases, based on the belief, and in one case a proof, that all 16 Wilf-class generating function coefficients can be represented as Stieltjes moment sequences.

The numerical estimates of growth constants and sub-dominant terms are given in tables 5 and 6.

Acknowledgements

References

[1] M. Albert, J. Pantone and V. Vatter, *On the growth of merges and staircases of permutation classes*, Rocky Mtn. J. Math. **49**(2) 355–367, (2019).

[2] M. Atapour and N. Madras, *Large deviations and ratio limit theorems for pattern-avoiding permutations,* Prob. and Comp. **23** 161–200, (2014).

[3] E. Babson and J. West, *The permutations $123p_4 \ldots p_t$ and $321p_4 \ldots p_t$ are Wilf-equivalent*, Graphs Combin. **16**(4) 373-380, (2000).

[4] J. Backelin, J. West and G. Xiu, *Wilf-equivalence for singleton classes*, Adv. in Appl. Math. **38**(20) 133–148, (2007).

[5] Y. Biers-Ariel, *Flexible schemes for pattern-avoiding permutations*, arXiv:1905.07283v2. Series in OEIS A116485.

[6] M. Bóna, *Exact enumeration of 1342-avoiding permutations: a close link with plane trees and planar maps*, J. Combin. Theory Ser. A **80** 257-272, (1997).

[7] M. Bóna, *The limit of a Stanley-Wilf sequence is not always rational and layered patterns beat monotone patterns*, J. Combin. Theory Ser. A **110** (2) 223-235, (2005).

[8] M. Bóna, *New records in Stanley-Wilf limits*, J. Combin. **28** (1) 75-85, (2007).

[9] A. Bostan, A. Elvey Price, A. J. Guttmann and J.-M. Maillard, *Stieltjes moment sequences for pattern-avoiding permutations*, Electron. J. Comb. **27**(4) #P4.20, (2020).

[10] R. E. Bryant, *Graph-based algorithms for Boolean function manipulation*, IEEE Trans. on Computers, **35** (8) 677–691, (1986).

[11] A. R. Conway, A. J. Guttmann and P. Zinn-Justin, *1324-avoiding permutations revisited*, Adv. in Appl. Math. **96** 312-333, (2018).

[12] H. Duminil-Copin and S. Smirnov, *The connective constant of the honeycomb lattice equals $\sqrt{2 + \sqrt{2}}$*, Ann. of Math. **175** (3) 1653-1665, (2012).

[13] A. R. Forsyth, Part III, Ordinary linear equations, vol. IV of *Theory of differential equations* Cambridge UP, (Cambridge), (1902).

[14] F. Gantmakher and M. Krein, *Sur les matrices completement non négatives et oscillatoires*, Compositio Mathematica **4** 445-476, (1937).

[15] S. Garrabrant and I. Pak, *Words in linear groups, random walks, automota and P-recursiveness*, J. Comb. Alg. **1**(2) 127-144, (2017).

[16] I. Gessel, *Symmetric functions and P-recursiveness*, J. Combin. Theory Ser. A **53** 257-285, (1990).

[17] A. J. Guttmann, in *Phase Transitions and Critical Phenomena,* vol 13, eds. C Domb and J. Lebowitz, Academic Press, London and New York, (1989).

[18] A. J. Guttmann, *Analysis of series expansions for non-algebraic singularities*, J. Phys. A: Math. Theor. **48** 045209, (33pp) (2015).

[19] A. J. Guttmann, *Series extension: predicting approximate series coefficients from a finite number of exact coefficients*, J. Phys A: Math. Theor. **49** 415002, (27pp) (2016).

[20] A. J. Guttmann and I. Jensen, Series Analysis. Chapter 8 of *Polygons, Polyominoes and Polycubes*, Lecture Notes in Physics **775**, ed. A. J. Guttmann, Springer, (Heidelberg), (2009).

[21] A. J. Guttmann and G. S. Joyce, *A new method of series analysis in lattice statistics*, J. Phys. A, **5** L81– 84, (1972).

[22] S. Haagerup, U. Haagerup and M. Ramirez-Solano, *A computational approach to the Thompson group F*, Int. J. Alg. and Comp. **25** 381-432, (2015).

[23] E. L. Ince, *Ordinary differential equations*, Longmans, Green and Co, (London), (1927).

[24] Y. Inoue, *Studies on Permutation Set Manipulation based on Decision Diagrams*, Doctor of Info. Sciences thesis, Hokkaido University, (2017). https://eprints.lib.hokudai.ac.jp/dspace/handle/2115/65366?locale=en&lang=en.

[25] Y. Inoue, *Paper in preparation*, (2022).

[26] Y. Inoue, T. Toda and S. Minato, *Implicit generation of pattern-avoiding permutations based on πDD,* TCS Technical Report TCS-TR-A-13.67, Hokkaido Univ. (2013).

[27] Y. Inoue and S. Minato, *An Efficient Method for Indexing All Topological Orders of a Directed Graph*, ISAAC 2014 Conference Proceedings, H.-K. Ahn and C.-S. Shin (Eds.) 103-114, (2014).

[28] W. Kuszmaul, *Fast algorithms for finding pattern avoiders and counting pattern occurrences in permutations*, Math. Comp. **87** 987-1011, (2018).

[29] S. Minato, *Zero-suppressed BDDs for set manipulation in combinatorial problems*, 30th Design Automation Conference, pp 272–277. ACM Press, (1993).

[30] S. Minato. *πDD: A New Decision Diagram for Efficient Problem Solving in Permutation Space*, Theory and Applications of Satisfiability Testing - SAT 2011 - 14th International Conference, SAT 2011, Ann Arbor, MI, USA, (2011). Proceedings, vol. 6695 of Lecture Notes in Computer Science, pp 90–104. Springer, Berlin, Heidelberg, (2011).

[31] A. Marcus and G. Tardos, *Excluded permutation matrices and the Stanley-Wilf conjecture*, J. Comb. Theory Ser. A. **107**(1) 153-160, (2004).

[32] G. B. Nguyen and N. Pétrélis, *A variational formula for the free-energy of the partially-directed polymer collapse*, J. Stat. Phys. **151** 1099-1120, (2013).

[33] OEIS Foundation Inc. (2014), The On-Line Encyclopedia of Integer Sequences, http://oeis.org.

[34] A. Regev, *Asymptotic values for degrees associated with strips of young diagrams*, Adv. in Math. **41**(2) 115–136, (1981).

[35] A. Reifegerste, *A generalization of Simion-Schmidt's bijection for restricted permutations*, Electron. J. Combin. **9**(2) #R14, (2002-3).

[36] Z. Stankova and J. West, *A new class of Wilf-equivalent permutations*, J. Alg. Combin. **15** 271-290, (2002).

[37] T.-J. Stieltjes, *Recherches sur les fractions continues,* Annales de la Faculté des sciences de Toulouse: Mathématiques. **8** (4) 1122, (1894).

[38] V. Vatter, *Permutation Classes*, in Handbook of Enumerative Combinatorics, ed. M. Bona, CRC Press, Boca Raton, Ch. 12 753–834, (2015).

Appendix A

In this appendix we give details of the analysis of the remaining five Wilf classes with a power-law singularity.

Av(25314)

The series was known up to, and including, terms of order x^{16}, given in the OEIS as sequence A256195. We have extended the known series by ten further terms, and the sequence of approximate coefficients and ratios by 100 further terms, using the method of series extension described above, based on third order differential approximants.

A plot of the ratios against $1/n$ is shown in Fig. 33, and we estimate the extrapolated limit at $1/n = 0$ to be $\mu = 12.6 \pm 0.1$. In Fig. 34 we show the linear intercepts, from which we give the more precise estimate $\mu = 12.57 \pm 0.01$. With quadratic intercepts we can sharpen this slightly to 12.5670 ± 0.0003. Using the central estimate $\mu = 12.5670$, we show estimates of the exponent g in Fig. 35 which we can linearly extrapolate, and give the estimate $g = -3.213 \pm 0.005$.

To increase confidence that we have the same pure power-law behaviour as prevails for $Av(12345)$, we estimated the exponent Δ, defined in eqn. (28), and found it to be extremely close to 1, consistent with pure power-law behaviour.

In Fig. 36, we show a plot of estimators of the exponent g which is independent of any estimate of μ. This extrapolates to a value consistent with the estimate just made assuming a value for μ. Linearly extrapolating this plot also gives the estimate $g = -3.213 \pm 0.005$.
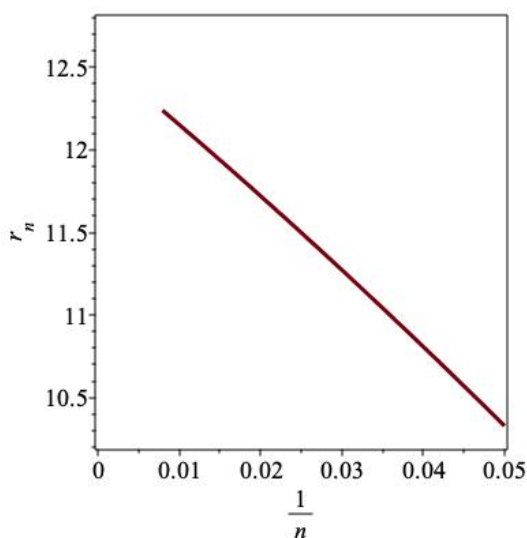
Figure 33: Ratios of $Av(25314)$ vs. $1/n$.
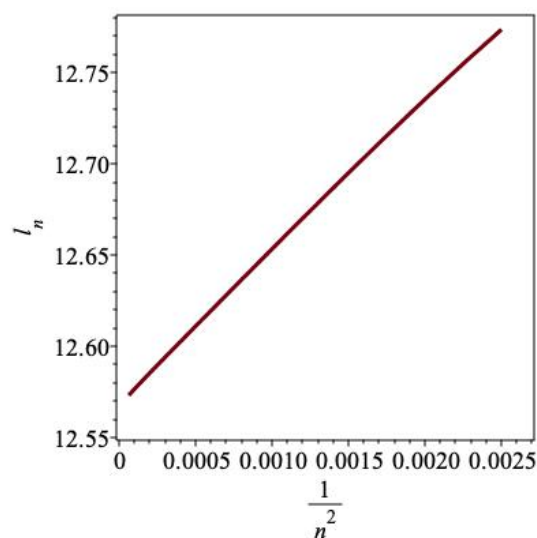
Figure 34: Linear intercepts of $Av(25314)$ vs. $1/n^2$.

We also fitted the ratio sequence to the assumed asymptotic form eqn. (29), and show the results in figs. 37 and 38 for μ and $\mu \cdot g$ respectively. Our previous estimate
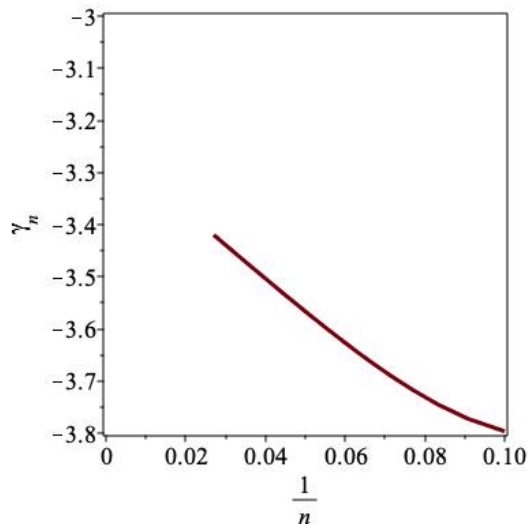
Figure 35: $Av(25314)$ exponent estimates assuming $\mu = 12.5670$.
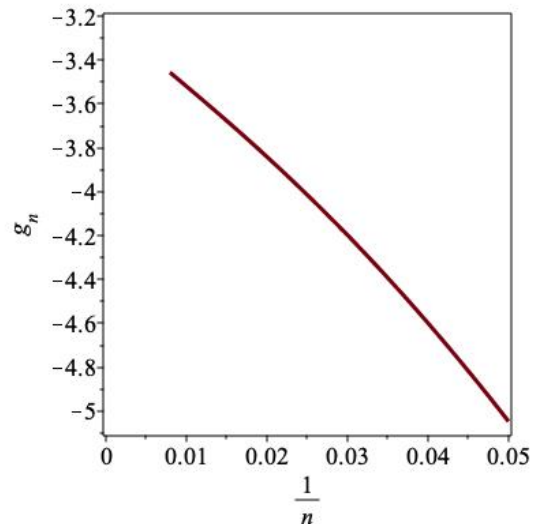
Figure 36: μ-independent $Av(25314)$ exponent estimates.

$\mu \approx 12.5670$ is well-supported, while $\mu \cdot g \approx -40.4$, so $g \approx -3.215$, both being consistent with our previous estimates.

We expect that the exponent is rational. The closest simple rational number is $3\frac{3}{14} = 3.21425\cdots$, and we offer this as our best guess as to the exact value. Using the central estimate of μ and the conjectured exponent, we can estimate the amplitude C, as we did for $Av(12345)$ in the previous subsection. In this way we find $C = 0.0164 \pm 0.0001$.

As we did for the analysis of $Av(12345)$, using the conjectured value of the exponent $g = -3\frac{3}{14}$ in this case, we can use direct fitting, as described in eqn. (25) to estimate C (and indeed μ). We did this and obtained the estimates $\mu \approx 12.5670$ and $C \approx 0.0164$. These are of course in complete agreement with the estimates obtained from the ratios.

We therefore conclude that

$$s_n(25314) \sim C\mu^n \cdot n^g,$$

with $\mu = 12.5670 \pm 0.0003$, $g = -3.214 \pm 0.006$, and $C = 0.0164 \pm 0.0001$. Our best guess is that $g = -3\frac{3}{14}$ exactly.

Lower bounds

Assuming that the Hankel determinants remain positive, then the ratios of the coefficients provide an increasing sequence of lower bounds. This gives the bound $\mu(25314) \geqslant 10.8809$. If the 100 predicted ratios are accepted, this improves the bound to $\mu(25314) \geqslant 12.240$.

If one constructs the continued fraction representation from the exact coefficients, (see Theorem 1 above), then the terms $\alpha_0 \ldots \alpha_{26}$ defined in Theorem 1 can be used to construct stronger bounds $(\sqrt{\alpha_n} + \sqrt{\alpha_{n-1}})^2$. In this way we obtain the bound $\mu(25314) \geqslant 12.46223$.
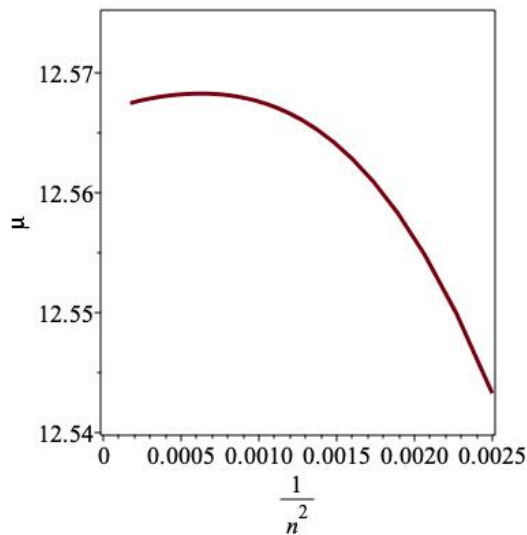
Figure 37: Estimate of growth constant μ vs. $1/n^2$.
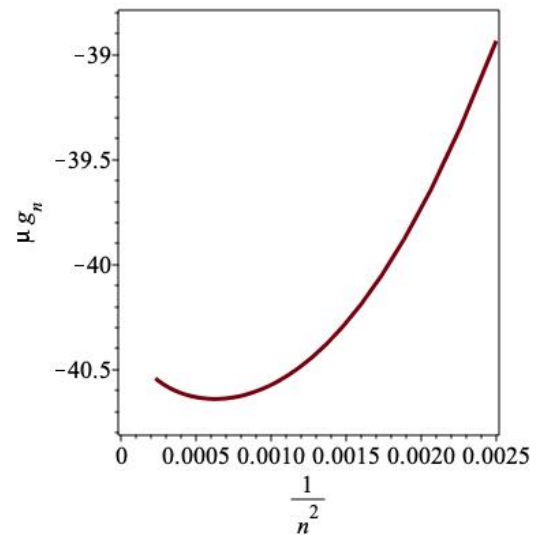
Figure 38: Estimate of $\mu \cdot g$ vs. $1/n^2$.

The sequence of lower bounds can also be extrapolated against $1/n^2$, shown in Fig. 39, and results in an estimate of μ consistent with, but less precise than, that obtained by the direct analysis of the original, extended series.
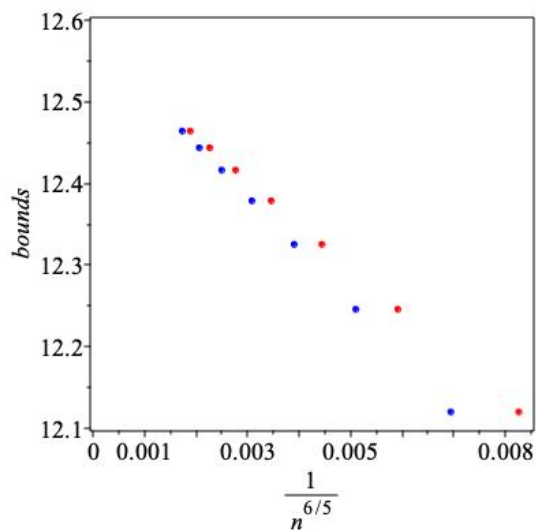
Figure 39: Stieltjes bounds vs. $1/n^2$ for $Av(25314)$.
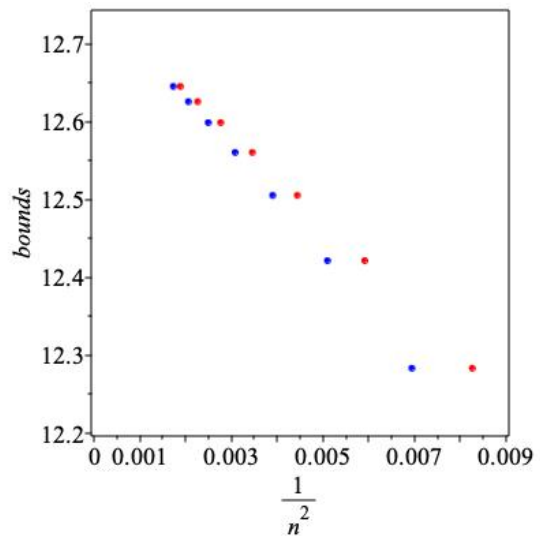
Figure 40: Stieltjes bounds vs. $1/n^2$ for $Av(31524)$.

Av(31524)

This series is now known up to, and including, terms of order x^{24}, given in the OEIS as sequence A256196 to order x^{16}. We have extended the sequence of ratios and coefficients by 100 further terms, as described above. The analysis parallels that just described above for the case of $Av(25314)$.

From the ratios, we estimate $\mu = 12.75 \pm 0.1$. From the linear intercepts we give the more precise estimate $\mu = 12.74 \pm 0.01$. Quadratic intercepts sharpen this to $\mu = 12.734 \pm 0.001$, and cubic intercepts give $\mu = 12.7344 \pm 0.0003$. Using the central estimate $\mu = 12.7344$, we estimate $g = -2.905 \pm 0.01$. Our estimate of the exponent g independent of any estimate of μ extrapolates to a value consistent with this estimate. As we consider it likely that the exponents are simple rationals, our best guess is $g = -2\frac{9}{10}$. We also made a 4-point fit to the ratios, and a 5-point fit, as defined in Sec. 7.2. These confirmed our estimates, above, of μ and g, and provided abundant evidence of a pure power-law singularity. As in the previous pattern, we estimated the amplitude C, and found $C = 0.00274 \pm 0.00005$.

As we did for the analysis of $Av(12345)$, using the conjectured value of the exponent $g = -2\frac{9}{10}$ in this case, we can use direct fitting, as described in eqn. (25) to estimate C (and indeed μ). We did this and obtained the estimates $\mu \approx 12.7344$ and $C \approx 0.000275$. These are of course in complete agreement with the estimates obtained from the ratios.

We therefore conclude that

$$s_n(31524) \sim C\mu^n \cdot n^g,$$

where $\mu = 12.7344 \pm 0.0003$, $g = -2.905 \pm 0.01$, and $C = 0.00274 \pm 0.00005$. Our best guess is that $g = -2\frac{9}{10}$ exactly.

Lower bounds

Assuming the observed positivity of the Hankel matrices persists, it follows that the coefficients form a Stieltjes moment sequence. The consequent log-convexity gives the bound $\mu(31524) \geqslant 10.9278$. If the 100 predicted coefficients are accepted, this improves the bound to $\mu(31524) \geqslant 12.4169$.

Constructing the continued fraction representation from the exact coefficients, (see Theorem 1 above), as in the previous pattern, then one finds $\mu(31524) \geqslant 12.6417$

The sequence of lower bounds can also be extrapolated against $1/n^2$, shown in Fig. 40, and results in an estimate of μ consistent with, but less precise than, that obtained by the direct analysis of the original, extended series.

Av(35214)

This series was known up to, and including, terms of order x^{14}, given in the OEIS as sequence A256197. We have extended the series by twelve terms. We have also extended the sequence of ratios and coefficients by 100 further ratios and coefficients, as described above, though the series is not quite as well-behaved, so our confidence bounds are wider. The analysis parallels that just described above for the case of $Av(31524)$.

From the ratios, we estimate $\mu = 13.3 \pm 0.1$. From the linear and quadratic intercepts we give the more precise estimate $\mu = 13.28 \pm 0.01$ and 13.275 ± 0.005 respectively. Using the central estimate $\mu = 13.275$, we estimate $g = -3.75 \pm 0.10$. Our estimate of the exponent g independent of any estimate of μ extrapolates to a value consistent with this estimate. We consider it likely that the exponents are simple rationals, so our best guess is $g = -3.75$. We also made 4-point and 5-point fits to the ratios, as above. These confirmed our estimates, above, of μ and g, and provided abundant evidence of a pure power-law singularity. As for the previous pattern, we estimated the amplitude C, and found $C = 0.0145 \pm 0.0015$. Note that this estimate assumes the central values for the parameters μ and g.

As we did for the analysis of $Av(12345)$, using the conjectured value of the exponent $g = -3.75$ in this case, we can use direct fitting, as described in eqn. (25) to estimate C (and indeed μ). We did this and obtained the estimates $\mu \approx 13.275$ and $C \approx 0.0143$. These are of course in complete agreement, within quoted uncertainties, with the estimates obtained from the ratios.

We therefore conclude $\mu = 13.275 \pm 0.005$, $g = -3.75 \pm 0.10$, and $C = 0.0145 \pm 0.0015$. That is to say

$$s_n(35214) \sim C\mu^n \cdot n^g,$$

where our best guess is that $g = -3.75$ exactly.

Lower bounds

Assuming that the coefficients form a Stieltjes moment sequence, the consequent log-convexity gives the bound $\mu(35214) \geqslant 11.2336$. If the 100 predicted coefficients are accepted, this improves the bound to $\mu(31524) \geqslant 12.8561$.

Constructing the continued fraction representation from the exact coefficients, (see Theorem 1 above), as above, one finds $\mu(35214) \geqslant 13.1159$.

The sequence of lower bounds can also be extrapolated against $1/n^2$, and results in an estimate of μ consistent with that obtained by the direct analysis of the original, extended series.

Av(43251)

This series was known up to, and including, terms of order x^{14}, given in the OEIS as sequence A256203. We have extended the series by twelve further terms. We have also extended the sequence of ratios by 100 further ratios, as described above. The analysis parallels those cases already discussed.

From the ratios, we estimate $\mu = 13.70 \pm 0.02$. From the linear and quadratic intercepts we give the more precise estimate $\mu = 13.703 \pm 0.001$. Using the central estimate $\mu = 13.703$, we estimate $g = -4.43 \pm 0.02$. Our estimate of the exponent g independent of any estimate of μ extrapolates to a value consistent with this estimate. We consider it likely that the exponents are simple rationals, and in this case appears to be $g = -4\frac{3}{7}$. We also made 4-point and 5-point fit to the ratios, as above. These confirmed our estimates, above, of

both μ and g, and provided abundant evidence of a pure power-law singularity. As for the previous pattern, we estimated the amplitude C, and found $C = 0.208 \pm 0.005$.

As we did for the analysis of $Av(12345)$, using the conjectured value of the exponent $g = -4\frac{3}{7}$ in this case, we can use direct fitting, as described in eqn. (25) to estimate C (and indeed μ). We did this and obtained the estimates $\mu \approx 13.703$ and $C = 0.206 \pm 0.005$ These are of course in complete agreement, within quoted uncertainties, with the estimates obtained from the ratios.

We therefore conclude $\mu = 13.703 \pm 0.001$, $g = -4.43 \pm 0.02$, and $C = 0.207 \pm 0.005$. That is to say

$$s_n(43251) \sim C\mu^n \cdot n^g,$$

where our best guess is that $g = -4\frac{3}{7}$ exactly.

Lower bounds

Assuming that the coefficients form a Stieltjes moment sequence, the consequent log-convexity gives the bound $\mu(43251) \geqslant 11.4821$. If the 200 predicted coefficients are believed, this improves the bound to $\mu(43251) \geqslant 13.4367$.

Constructing the continued fraction representation from the exact coefficients, (see Theorem 1 above), as above, then one finds $\mu(43251) \geqslant 13.5111$.

This sequence of lower bounds can also be extrapolated against $1/n^2$, and results in an estimate of μ consistent with that obtained by the direct analysis of the original, extended series.

Av(34215)

This series was known up to, and including, terms of order x^{14}, given in the OEIS as sequence A256205. We have extended the series by twelve further terms. We have also extended the sequence of ratios by 200 further ratios, as described above. We were able to extend the series by 200 ratios rather than the extension by 100 ratios of the preceding sequences simply because the computed error in the coefficients increased more slowly with increasing order of the coefficients in this case than in other cases. We do not know why. The analysis parallels that described above, though the series is slightly less well-behaved, so the uncertainties in our estimates are greater.

From the ratios, we estimate $\mu = 13.97 \pm 0.05$. From the linear intercepts we give the more precise estimate $\mu = 13.95 \pm 0.01$, and from quadratic fits and 4-point fits we make a slightly lower estimate, $\mu = 13.945 \pm 0.008$. Using the central estimate $\mu = 13.945$, we estimate $g = -4.67 \pm 0.01$. Our estimate of the exponent g independent of any estimate of μ extrapolates to a similar value, though less precisely.

Assuming $g = -4\frac{2}{3}$ exactly, then allowing for the error estimate in μ, we find $C = 0.375 \pm 0.08$, where the bulk of the uncertainty stems from the uncertainty in μ.

We therefore conclude $\mu = 13.945 \pm 0.008$, $g = -4.67 \pm 0.01$, $C = 0.375 \pm 0.08$. That is to say

$$s_n(34215) \sim C\mu^n \cdot n^g.$$

Our best guess for the exact value of the exponent g is $g = -4\frac{2}{3}$. Note that the growth rate is smaller than that of $Av(53124)$, even though all known coefficients of $Av(34215)$ are greater than those of $Av(53124)$. For sufficiently high order, this pattern must of course reverse.

Lower bounds

Assuming that the coefficients form a Stieltjes moment sequence, the consequent log-convexity gives the bound $\mu(34215) \geqslant 11.6002$. If the 200 predicted coefficients are believed, this improves the bound to $\mu(34215) \geqslant 13.6611$.

Constructing the continued fraction representation from the exact coefficients, (see Theorem 1 above), as above, one finds $\mu(34215) \geqslant 13.7131$.

This sequence of lower bounds can also be extrapolated against $1/n^2$, and results in an estimate of μ consistent with, but less precise than, that obtained by the direct analysis of the original, extended series.

Appendix B

In this appendix we give details of the analysis of the remaining nine Wilf classes with a stretched-exponential singularity.

Av(53124)

This series was known up to, and including, terms of order x^{14}, given in the OEIS as sequence A256199. We have extended the series by eleven further terms.

The analysis parallels that described above for the case of $Av(12453)$, though this series does not behave as nicely as does the series $Av(12453)$, presumably because we have significantly fewer terms. Accordingly, we have been able to extend the number of approximate coefficients, and ratios, by 100, rather than 400 in the previous case.

The ratios, when plotted against $1/n$ display some curvature which is not disappearing as n increases. This allows us to estimate $\mu > 14.0$. Curvature in this ratio plot is usually a hallmark of a stretched-exponential singularity, as discussed above. We investigate this further by checking if the sequence $n^2(r_n/r_{n-1} - 1)$ diverges with n, as explained in the discussion around eqn. (13). The relevant plot is shown in Fig. 41, and is clearly diverging as n increases.

If we plot the ratios against $1/n^{3/4}$, see Fig. 42 the plot is visually linear. This would imply a stretched-exponential term of the form $\mu_1^{n^{1/4}}$, which is not an exponent we have previously encountered. Extrapolating this gives the estimate $14.2 < \mu < 14.3$.

The permutation pattern 53124 is a simple decreasing sequence (531) followed by an increasing sequence, (24), so there is nothing there that would suggest a stretched exponential term. The previous pattern we have studied $Av(12453)$ is similar, in that it is an increasing sequence (1245) followed by a decreasing sequence (53). Most of the sequences we study here that display clear evidence of a stretched-exponential term contain the pattern 1324, whereas this does not.

If we had a pure power law, linear intercepts would eliminate the $O(1/n)$ term in the expression for the ratios, and the linear intercepts would behave as $l_n \sim \mu(1 + c/n^2)$. A plot of the linear intercepts against $1/n^2$ is shown in Fig. 43, and it is clear that this is far from linear! This is strong evidence against a pure power-law singularity. However plotting these linear intercepts against $1/n^{3/4}$, as appropriate, allows us to estimate $\mu = 14.24 \pm 0.05$.
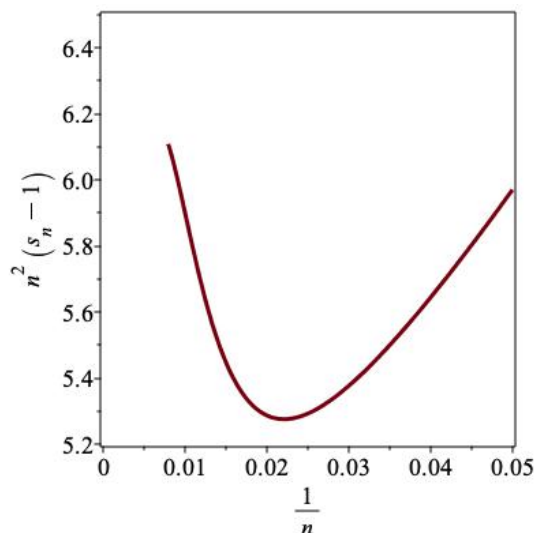
Figure 41: $n^2(s_n - 1)$ vs. $1/n$, showing divergence.
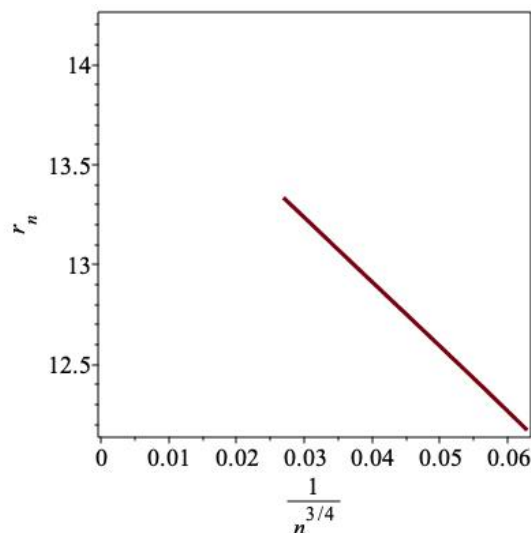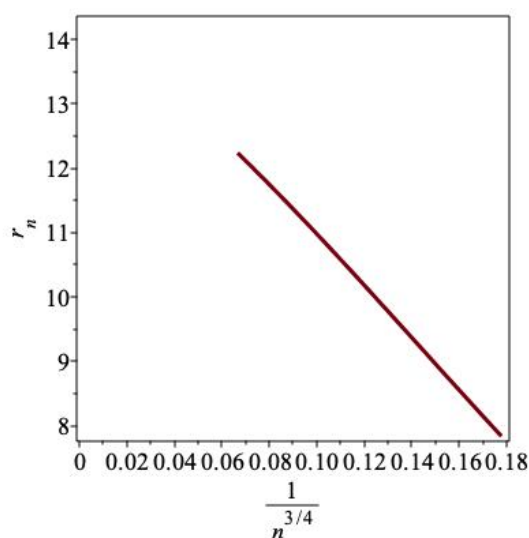
Figure 42: $Av(53124)$ ratios vs. $n^{-3/4}$.

As in the previous pattern, we can form estimates for the exponent σ assuming the value of μ, and, less precisely, without assuming μ. The result of doing this is shown in figs 44 and 45 respectively, where the upper and lower curves in both figures represent the results of using the two different methods for estimating σ, as explained in the previous subsection. It can be seen that these plots lend support to the estimate $\sigma = 1/4$, originally conjectured based on linearity of the ratio plots.

We tried a variety of other methods to estimate the various parameters, as discussed in the previous subsection, but these were inconclusive. Accordingly, while $\sigma = 1/4$ is our candidate for the most likely exact value, we cannot totally rule out $\sigma = 1/3$, as found for $Av(12453)$. This is reflected in the quoted error bar, which should be interpreted as a confidence limit.

The uncertainty in our estimate of μ prevents us from estimating the stretched-exponential growth constant μ_1 or the exponent g with useful precision. We therefore conclude $\mu = 14.24 \pm 0.05$, $\sigma = 0.25 \pm 0.1$. That is to say

$$s_n(53124) \sim C\mu^n \cdot \mu_1^{n^\sigma} \cdot n^g,$$

with μ_1 C and g unknown.
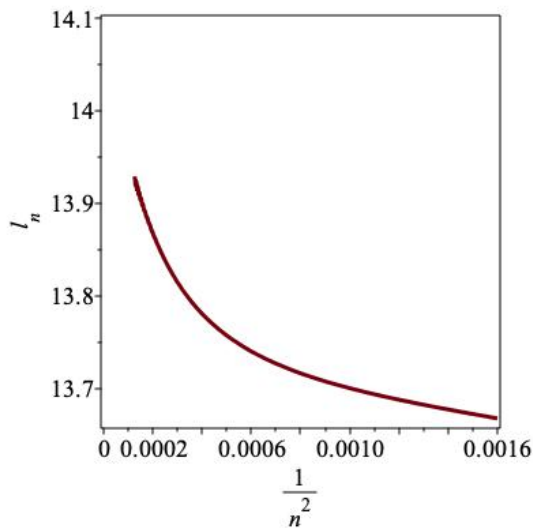
Figure 43: Linear intercepts of $Av(53124)$ vs. $1/n^2$.
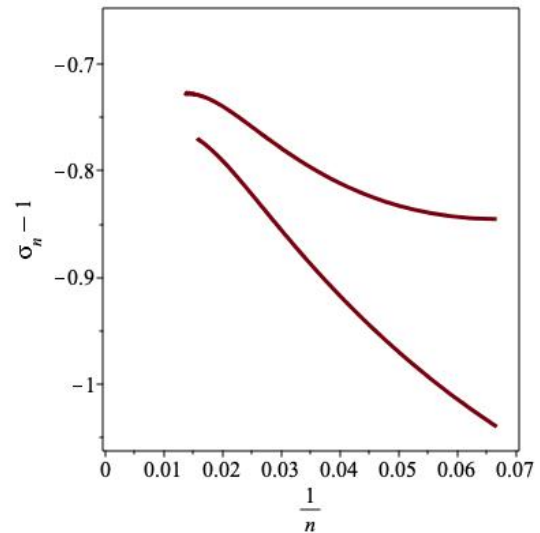
Figure 44: Estimate of exponent σ, assuming μ vs. $1/n$.
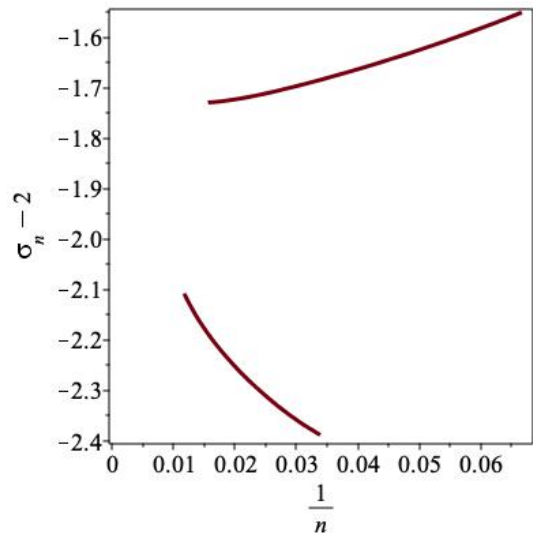
Figure 45: Estimate of exponent σ, independent of μ vs. $1/n$.
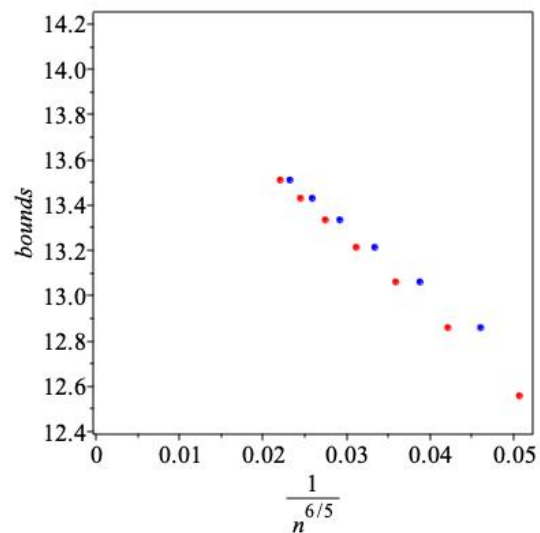
Figure 46: Stieltjes bounds vs. $1/n^{6/5}$.

Lower bounds

Assuming that the coefficients form a Stieltjes moment sequence, the consequent log-convexity gives the bound $\mu(53124) \geqslant 11.3441$. If the 100 predicted coefficients are accepted, this improves the bound to $\mu(53124) \geqslant 13.3481$.

Constructing the continued fraction representation from the exact coefficients, (see Theorem 1 above), as above, one finds $\mu(53124) \geqslant 13.5836$.

In Fig. 46 we show these Stieltjes bounds plotted against the appropriate power of n.

It can be seen that they can be extrapolated approximately linearly to the top-leftmost point of the plot, at the estimated value $\mu = 14.24$.

Av(32541)

This series was also known up to, and including, terms of order x^{14}, given in the OEIS as sequence A256204. We have extended the series by thirteen further terms. We have also extended the sequence of ratios by 100 further ratios, as described above. The analysis parallels that just described above for the case of $Av(35124)$.

In Fig. 47 we show the ratios plotted against $1/n$. This plot is slightly concave, and can be crudely extrapolated to give the estimate $\mu \approx 14.3$. If we plot the ratios against $1/n^{3/4}$, see Fig. 48 the plot is visually linear. This would imply a stretched-exponential term of the form $\mu_1^{n^{1/4}}$. Extrapolating this gives the estimate $\mu \approx 14.35$.
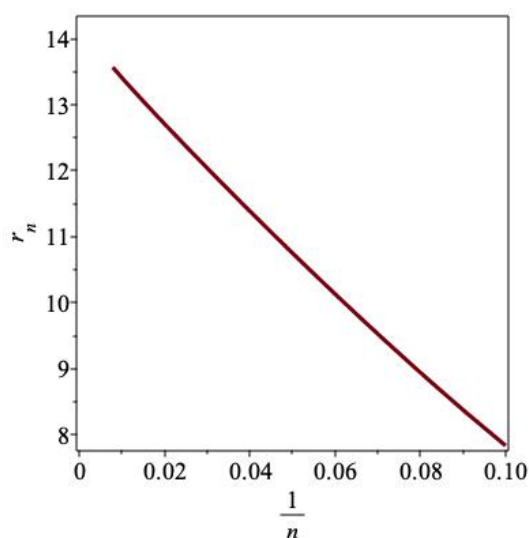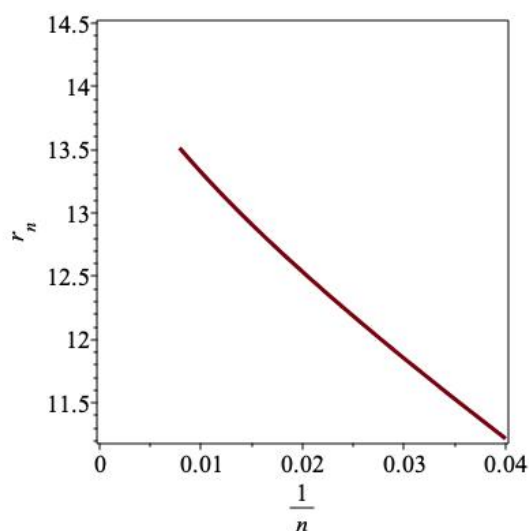

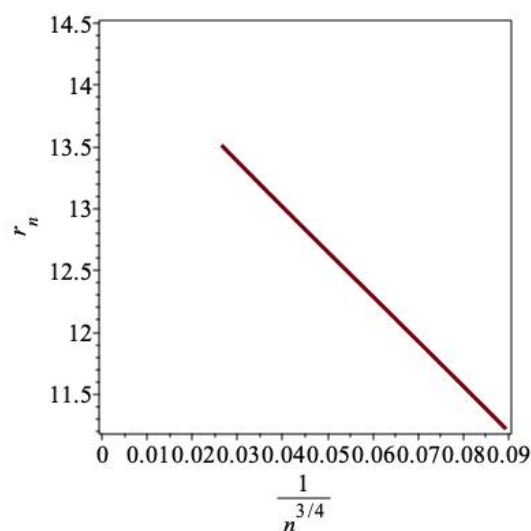Figure 47: Ratios of $Av(32541)$ vs. $1/n$. Figure 48: $Av(53124)$ ratios vs. $n^{-3/4}$.

As in the previous pattern, we can form estimates for the exponent σ assuming the value of μ, and, less precisely, without assuming μ. The result of doing this is shown in figs 53 and 54 respectively, where the upper and lower curves in both figures represent the results of using two different methods for estimating σ, as explained in the previous subsection. It can be seen that these plots are somewhat inconclusive, suggesting estimates of σ in the range $(1/5, 1/3)$, but with $\sigma = 1/4$ as the central estimate. Thus we take this as our most likely exact value, but quote our estimate as $\sigma = 0.27 \pm 0.07$.

Assuming $\sigma = 1/4$, we can fit to the expression for the logarithm of coefficients as described around eqn. (20) to estimate the other parameters. In this way we estimate $\mu \approx 14.30$, $\log \mu_1 \approx -5$, and $g \approx -2$.

With $\sigma = 1/3$, we find $\mu \approx 14.35$, $\log \mu_1 \approx -2.2$, and $g \approx -3$.

We have also estimated these parameters by fitting the *ratios* to the expected form, as explained in the description of eqn. (23). This produces similar estimates.
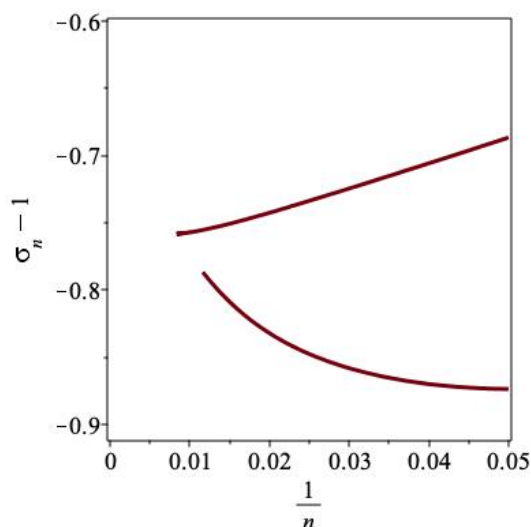
Figure 49: Estimate of exponent σ, assuming μ vs. $1/n$.
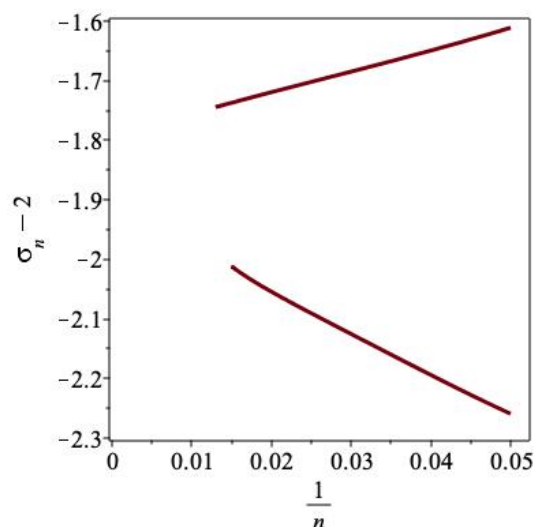
Figure 50: Estimate of exponent σ, independent of μ vs. $1/n$.

As in the previous pattern considered, the uncertainty in the estimate of μ prevents us from estimating the stretched-exponential growth constant μ_1 or the exponent g with useful precision, as their estimation depends sensitively on the value of the exponent σ.

We therefore conclude $\mu = 14.32 \pm 0.04$, $\sigma = 0.27 \pm 0.07$, with $\sigma = 1/4$ or $1/3$ as the most likely values. That is to say

$$s_n(32541) \sim C\mu^n \cdot \mu_1^{n^\sigma} \cdot n^g.$$

If $\sigma = 1/4$, then we estimate $\mu_1 \approx 0.007$, and $g \approx -2$. If $\sigma = 1/3$, then we estimate $\mu_1 \approx 0.11$, and $g \approx -3$.

Lower bounds

Assuming that the coefficients form a Stieltjes moment sequence, the consequent log-convexity gives the bound $\mu(32541) \geqslant 11.5813$. If the 100 predicted coefficients are believed, this improves the bound to $\mu(32541) \geqslant 13.5669$.

Constructing the continued fraction representation from the exact coefficients, (see Theorem 1 above), as above, one finds $\mu(32541) \geqslant 13.8447$.

This sequence of lower bounds can also be extrapolated against $1/n^{6/5}$, shown in Fig. 55 and results in an estimate of μ consistent with that obtained by the direct analysis of the original, extended series.

Av(35124)

This series was known up to, and including, terms of order x^{14}, given in the OEIS as sequence A256198. We have extended the series by thirteen further terms. We have also

extended the sequence of ratios by 100 further ratios, as described above. The analysis parallels that just described above for the case of $Av(32541)$.

In Fig. 51 we show the ratios plotted against $1/n$, which appears to be concave. If we plot the ratios against $1/n^{3/4}$, see Fig. 52 the plot is visually linear. This would imply a stretched-exponential term of the form $\mu_1^{n^{1/4}}$, just as observed for $Av(53124)$. Extrapolating this gives the estimate $\mu \approx 14.50$.

If we had a pure power law, linear intercepts would eliminate the $O(1/n)$ term in the expression for the ratios, and the linear intercepts would behave as $l_n \sim \mu(1 + c/n^2)$. A plot of the linear intercepts against $1/n^2$ displays considerable curvature, which is further evidence against simple power-law behaviour. However plotting the linear intercepts against $1/n^{3/4}$, as appropriate, allows us to estimate $\mu = 14.54 \pm 0.03$.

Figure 51: Ratios of $Av(35124)$ vs. $1/n$. Figure 52: $Av(35124)$ ratios vs. $1/n^{3/4}$.

As in the previous pattern, we can form estimates for the exponent σ assuming the value of μ, and, less precisely, without assuming μ. The result of doing this is shown in figs 53 and 54 respectively, where the upper and lower curves in both figures represent the results of using the two different methods for estimating σ, as explained in the previous subsection. It can be seen that these plots lend support to the estimate $\sigma = 1/4$, based on linearity of the ratio plots.

As in the previous pattern considered, the uncertainty in the estimate of μ prevents us from estimating the stretched-exponential growth constant μ_1 or the exponent g with useful precision. We therefore conclude $\mu = 14.54 \pm 0.03$, $\sigma = \frac{1}{4}$. That is to say

$$s_n(35124) \sim C\mu^n \cdot \mu_1^{n^\sigma} \cdot n^g.$$

Unlike the previous two patterns, the value $\sigma = 1/4$ seems much less equivocal than in those cases, so we do not quote error estimates in this case, but remark that while this is our most favoured value, it is not impossible that σ is as large as $1/3$.
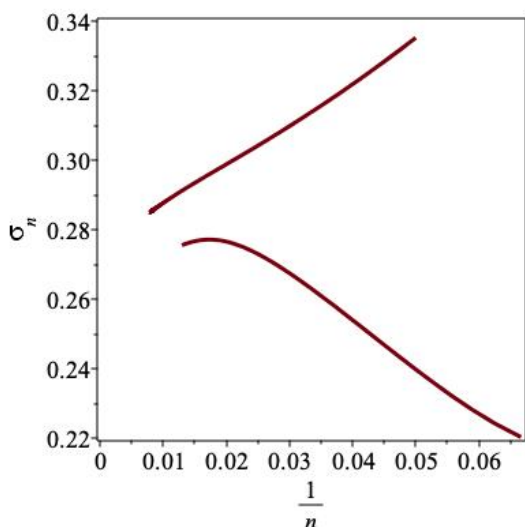
Figure 53: Estimate of exponent σ, assuming μ vs. $1/n$.
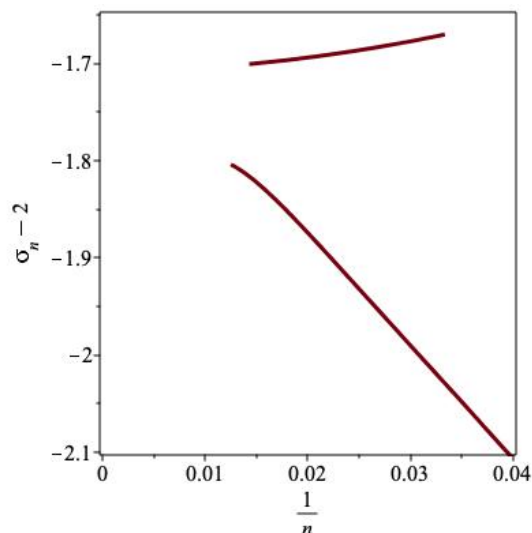
Figure 54: Estimate of exponent σ, independent of μ vs. $1/n$.

Lower bounds

Assuming that the coefficients form a Stieltjes moment sequence, the consequent log-convexity gives the bound $\mu(35124) \geqslant 11.4025$. If the 100 predicted coefficients are accepted, this improves the bound to $\mu(35124) \geqslant 13.5150$.

Constructing the continued fraction representation from the exact coefficients, (see Theorem 1 above), as above, then one finds $\mu(35124) \geqslant 13.7433$.

This sequence of lower bounds can also be extrapolated against $1/n^{6/5}$, as shown in Fig. 56 and results in an estimate of μ consistent with that obtained by the direct analysis of the original, extended series.

Av(42351)

This series was known up to, and including, terms of order x^{15}, given in the OEIS as sequence A256200. We have extended the series by twelve further terms. We have also extended the sequence of ratios, and the coefficient sequence, by 100 further terms, as described above. The analysis parallels those cases already discussed.

The ratio plots of the known series displays curvature when plotted against $1/n$, see Fig. 57, and this curvature persists when we include the extrapolated ratios. From the permutation pattern 41325 (which is in the same Wilf class as this permutation), we see the characteristic 1324 pattern that is a hallmark of a stretched exponential term.

The curvature disappears when the ratios are plotted against $1/n^{2/3}$, see Fig. 58. This implies a singularity structure with a stretched exponential term. As the pattern 35241 contains a sub-pattern qualitatively similar to 4231, believed to have stretched-exponential asymptotics, this is unsurprising, and, indeed, expected.

The ratio plot against $1/n^{2/3}$ is seen to be visually linear, and extrapolates to $\mu =$
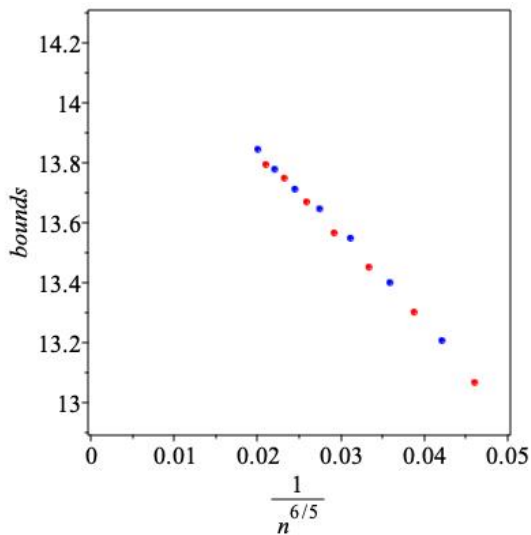
Figure 55: Stieltjes bounds for $Av(32541)$ vs. $1/n^{6/5}$.
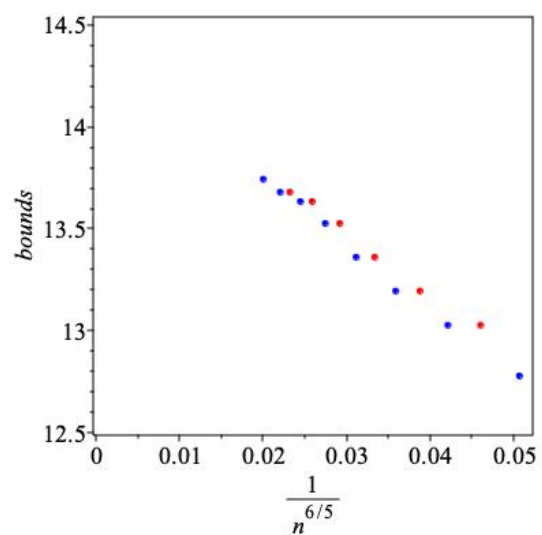
Figure 56: Stieltjes bounds for $Av(35124)$ vs. $1/n^{6/5}$.
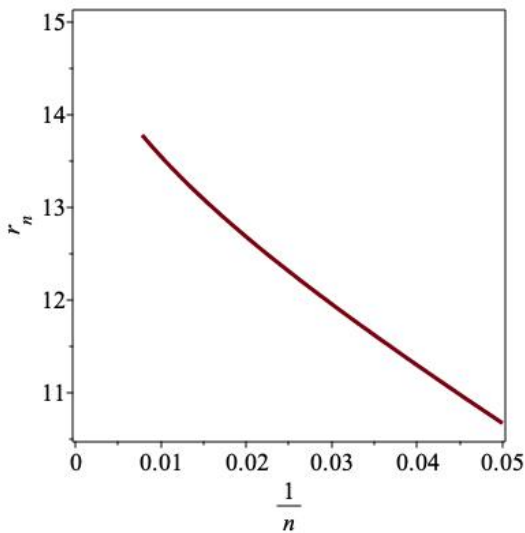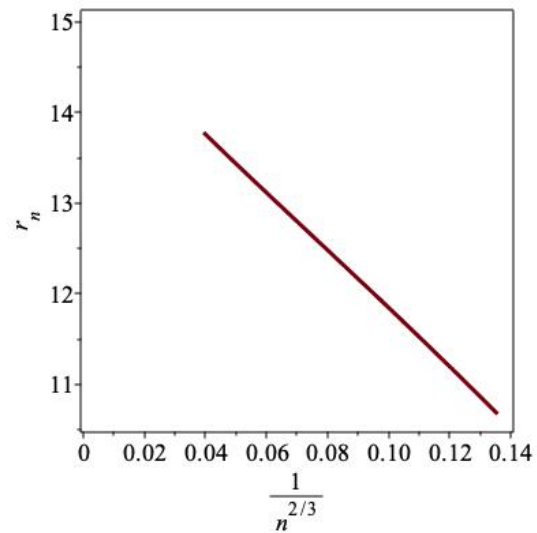

Figure 57: Ratios of $Av(42351)$ vs. $1/n$.

Figure 58: $Av(42351)$ ratios vs. $1/n^{2/3}$.

15.1 ± 0.1. Note that this linearity implies a stretched-exponential term with exponent $\sigma = 1/3$. Linear intercepts, which eliminate the competing $O(1/n)$ term, allow this estimate to be sharpened to $\mu = 15.10 \pm 0.05$.

Assuming $\mu = 15.10$, as shown above we can estimate the value of σ using the two methods we have previously discussed. The estimates of σ from these two methods are shown Fig. 59, and are consistent with our conjectured value, σ is $1/3$. We can also estimate σ less precisely without assuming the value of μ. Again we utilise the two distinct methods discussed above for this estimate. These estimates of σ are shown Fig. 60, and

are also consistent with our conjectured value, $\sigma = 1/3$.

From the expected asymptotic behaviour of the ratios in this case, shown in eqn. (11), we can try and estimate the subdominant growth constant μ_1 and exponent g. We can use eqn. (19) and extrapolate against $1/n$, and estimate the quantity $\sigma \log \mu_1$ as -6.75 ± 0.45, where we assume $\sigma = 1/3$, and the uncertainty quoted arises from the uncertainty associate with the estimate of μ. This implies $\mu_1 = 0.0012 \pm 0.0006$. We emphasis that this is a rather imprecise estimate, and should be considered to be more an order-of-magnitude estimate than anything more.

We obtained an alternative estimate of μ_1 by direct fitting to the unknown parameters C, $\log \mu_1$ and g in eqn. (20), assuming the central estimate of μ. In this way we estimate $g = -1.25 \pm 0.25$, and obtained a similar estimate of μ_1 to that just quoted. The estimate of C is very sensitive to the estimate of μ, and we can only conclude $1 < C < 2$.

We therefore conclude that $s_n(42351) \sim C \cdot \mu^n \cdot \mu_1^{n^\sigma} \cdot n^g$, with $\mu = 15.10 \pm 0.05$, $\sigma = 1/3$, $\mu_1 = 0.0012 \pm 0.0006$, $g = -1.25 \pm 0.25$, and $1 < C < 2$.
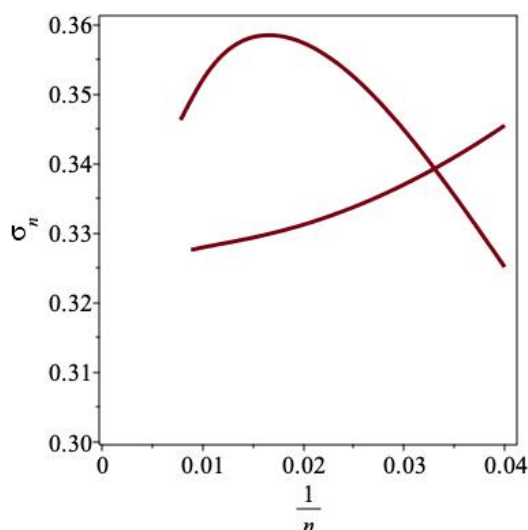
Figure 59: Estimators of σ for $Av(42351)$ vs. $1/n$ assuming $\mu = 15.0$.
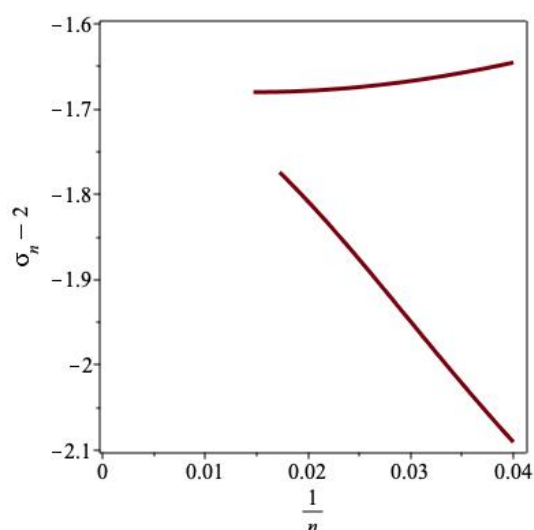
Figure 60: Estimators of $2 - \sigma$ for $Av(42351)$ without assuming μ.

Lower bounds

Assuming that the coefficients form a Stieltjes moment sequence, the consequent log-convexity gives the bound $\mu(42351) \geqslant 11.4884$. If the 100 predicted coefficients are believed, this improves the bound to $\mu(42351) \geqslant 13.7711$.

Constructing the continued fraction representation from the exact coefficients, (see Theorem 1 above), as above, then one finds $\mu(42351) \geqslant 14.0314$.

This sequence of lower bounds can also be extrapolated against $1/n$, see Fig. 61 and results in an estimate of μ consistent with that obtained by the direct analysis of the original, extended series.
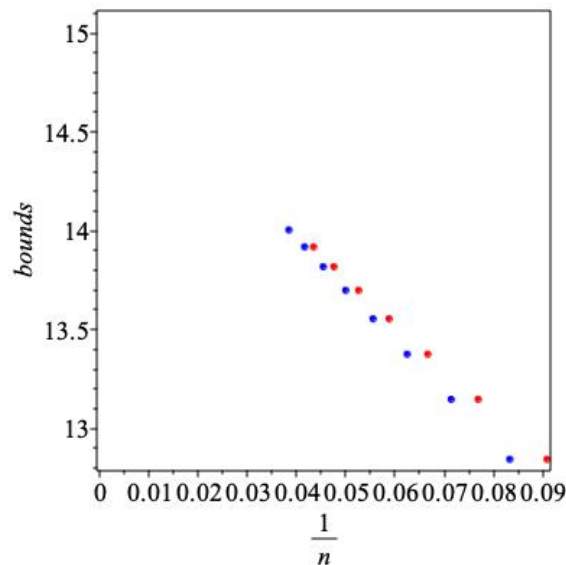
Figure 61: Stieltjes bounds for $Av(42351)$ vs. $1/n^{6/5}$.

Av(42315)

This series was known up to, and including, terms of order x^{14}, given in the OEIS as sequence A256206. We have extended the series by twelve further terms. We have also extended the sequence of ratios (and coefficients) by 200 further ratios (and coefficients), as described above.

The ratios, when plotted against $1/n$, display curvature, which disappears when the ratios are plotted against $1/n^{3/4}$, see Fig. 62. It appears to be linear, and extrapolates to $\mu = 15.4 \pm 0.2$. This linearity implies a stretched-exponential term with exponent $\sigma = 1/4$. Linear intercepts, which eliminate the competing $O(1/n)$ term, allow this estimate to be sharpened to $\mu = 15.40 \pm 0.1$.

Assuming $\sigma = 1/4$, one can fit sequences of four successive ratios to the asymptotic form given by eqn. (23), and also fit four successive coefficients to the coefficient asymptotic form eqn. (20).

From the fit to the ratios, we find $\mu = 15.40 \pm 0.04$, and $\sigma \log \mu_1 = -2.3 \pm 0.1$, so $\mu_1 = 0.0001 \pm 0.00005$.

From the fit to the logarithm of the coefficients we find $\log C = 4.5 \pm 0.2$, so $C = 90 \pm 16$, and $\log \mu \approx 2.736$, so $\mu \approx 15.42$.

We combine these various estimates of μ to give the final estimate $\mu = 15.40 \pm 0.04$.

We directly estimate σ assuming the value of μ by two methods. The first estimator is given by eqn. (15), the second by calculating the gradient of the log-log plot obtained from eqn(16). These estimators are shown in Fig. 64. One can also estimate the value of σ without any estimate of μ, by calculating the local gradient of the log-log plots of the two estimators given by eqn. (17) and eqn. (18). These estimators are shown in Fig. 65. Both pairs of plots give results consistent with our estimate $\sigma = 1/4$.
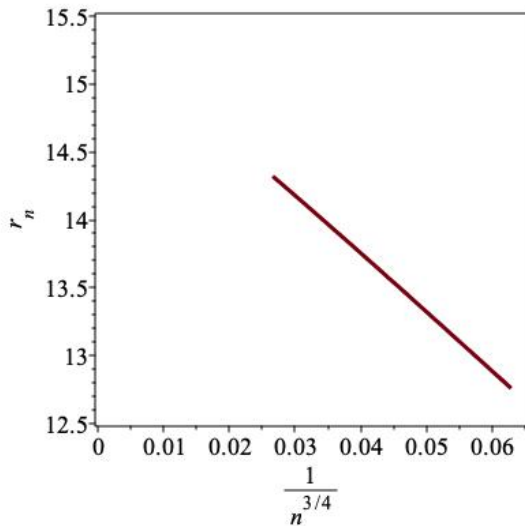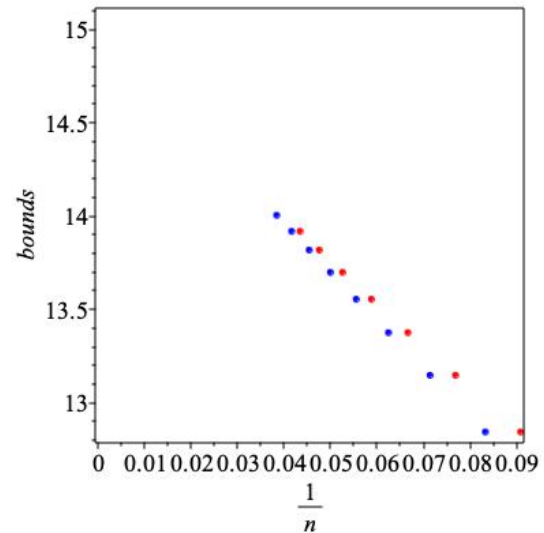
Figure 62: $Av(42315)$ ratios vs. $1/n^{3/4}$.

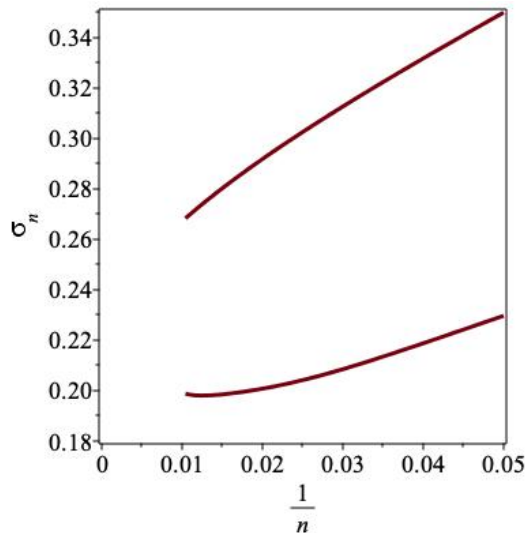Figure 63: Stieltjes bounds for $Av(42315)$ vs. $1/n^{6/5}$.

Figure 64: Estimate of exponent σ vs. $1/n$, assuming μ. First method, upper curve, second method, lower curve.
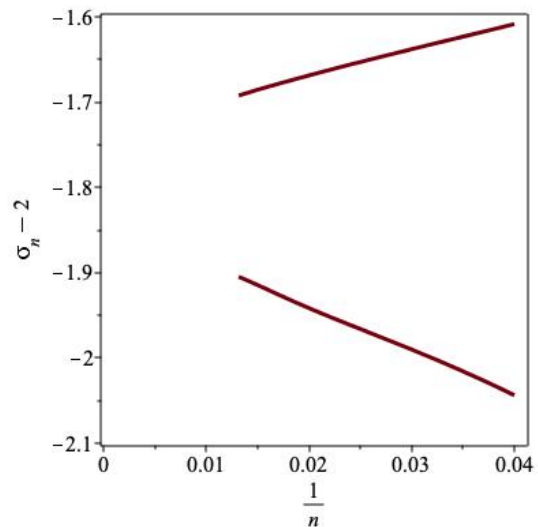

Figure 65: Estimate of exponent $\sigma - 2$ vs. $1/n$ without knowing μ. First method, upper curve, second method, lower curve.

We therefore conclude that $s_n(42315) \sim C \cdot \mu^n \cdot \mu_1^{n^{1/4}} \cdot n^g$, with $\mu = 15.40 \pm 0.04$, $\sigma = 1/4$, $\mu_1 = 0.0001 \pm 0.00005$, and $C = 90 \pm 16$. We give no estimate of the exponent g.

Lower bounds

Assuming that the coefficients form a Stieltjes moment sequence, the consequent log-convexity gives the bound $\mu(42315) \geqslant 11.8117$. If the 200 predicted coefficients are

believed, this improves the bound to $\mu(42315) \geqslant 14.7160$.

Constructing the continued fraction representation from the exact coefficients, (see Theorem 1 above), as in the previous PAP, one finds $\mu(42315) \geqslant 14.5633$.

This sequence of lower bounds can be extrapolated against $1/n^{6/5}$, shown in Fig. 63 and results in an estimate of $\mu \approx 15.4$ consistent with that obtained by the direct analysis of the original, extended series.

Av(35241)

This series was known up to, and including, terms of order x^{14}, given in the OEIS as sequence A256201. We have extended the series by twelve further terms. We have also extended the sequence of ratios approximately by 100 further coefficients and ratios, as described above.

The ratios, when plotted against $1/n$, display curvature, which disappears when the ratios are plotted against $1/n^{2/3}$, see Fig. 66. This implies a singularity structure with a stretched exponential term. As the pattern 35241 contains a sub-pattern qualitatively similar to 4231, believed to have stretched-exponential asymptotics, this is unsurprising, and, indeed, expected.

The ratio plot against $1/n^{2/3}$ is seen to be visually linear, and extrapolates to $\mu = 16.2 \pm 0.2$. This linearity implies a stretched-exponential term with exponent $\sigma = 1/3$. Linear intercepts, which eliminate the competing $O(1/n)$ term, allow this estimate to be sharpened to $\mu = 16.2 \pm 0.1$.

Assuming $\sigma = 1/3$, one can fit sequences of four successive ratios to the asymptotic form given by eqn. (23), and also fit four successive coefficients to the asymptotic form eqn. (20).

From the fit to the ratios, we find $\mu = 16.20 \pm 0.05$, and $\sigma \log \mu_1 = -3.1 \pm 0.2$, so $\mu_1 = 0.00009 \pm 0.00004$.

From the fit to the logarithm of the coefficients we find $\log C = 2.9 \pm 0.4$, so $C = 18 \pm 9$.

We combine these various estimates of μ to give the final estimate $\mu = 16.20 \pm 0.05$.

We can directly estimate σ assuming the value of μ by two methods, as described above. The first estimator is given by eqn. (15), the second by calculating the gradient of the log-log plot obtained from eqn(16). These estimators are shown in Fig. 67. One can also estimate the value of σ without any estimate of μ, by calculating the local gradient of the log-log plots of the two estimators given by eqn. (17) and eqn. (18). These estimators are shown in Fig. 68. Both pairs of plots give results consistent with our estimate $\sigma = 1/3$.

We therefore conclude that $s_n(35241) \sim C \cdot \mu^n \cdot \mu_1^{n^{\sigma}} \cdot n^g$, with $\mu = 16.20 \pm 0.05$, $\sigma = 1/3$, $\mu_1 \approx 0.00009$, and $C = 18 \pm 9$. We give no estimate of the exponent g.

Lower bounds

Assuming that the coefficients form a Stieltjes moment sequence, the consequent log-convexity gives the bound $\mu(35241) \geqslant 11.6779$. If the 100 predicted coefficients are believed, this improves the bound to $\mu(35241) \geqslant 14.4634$.
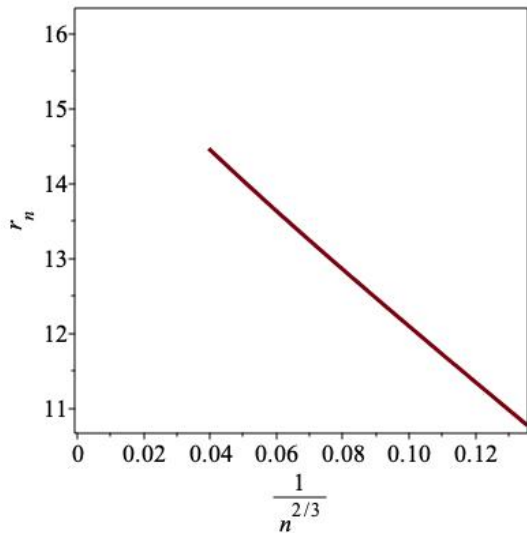
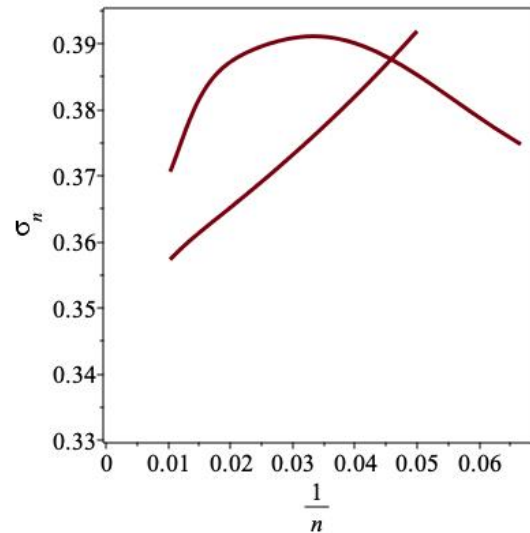Figure 66: f $Av(35241)$ ratios vs. $1/n^{2/3}$.

Figure 67: Estimators of $1 - \sigma$ for $Av(35241)$ vs. $1/n$.

Constructing the continued fraction representation from the exact coefficients, (see Theorem 1 above), as above, then one finds $\mu(35241) \geqslant 14.6253$.

This sequence of lower bounds can be extrapolated against $1/n$, shown in Fig. 69, and results in an estimate of $\mu \approx 16$, consistent with that obtained by the direct analysis of the original, extended series.
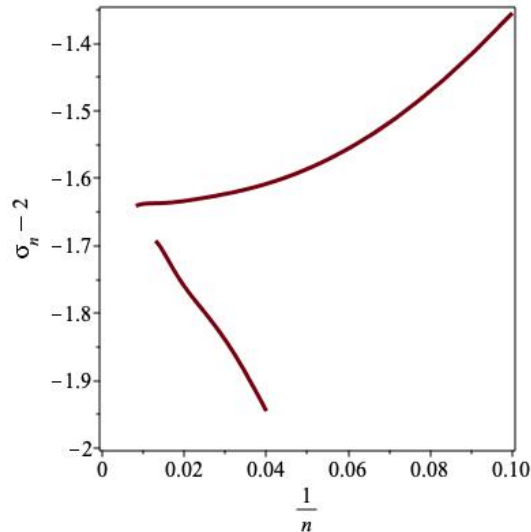
Figure 68: Estimate of exponent σ vs. $1/n$, without μ. First method, upper curve, second method, lower curve.
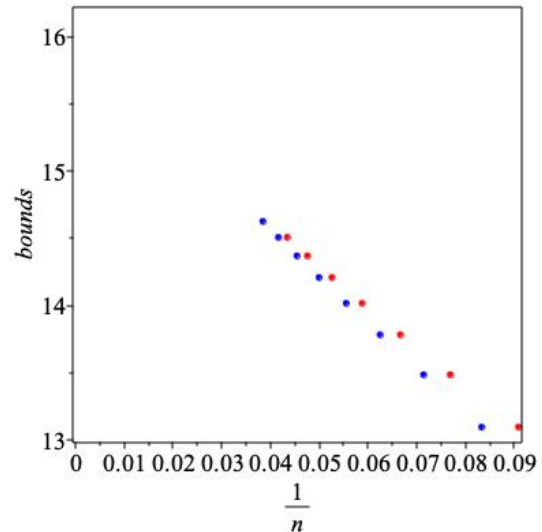
Figure 69: Stieltjes bounds on μ for $Av(35241)$.

Av(53241)

This series was known up to, and including, terms of order x^{14}, given in the OEIS as sequence A256202. We have extended the series by twelve further terms. We have also extended the sequence of ratios, and coefficients, by 100 approximate further terms as described above.

The ratios, when plotted against $1/n$, display curvature which disappears when the ratios are plotted against $1/n^{1/2}$. This implies a singularity structure with a stretched exponential term. The corresponding ratio plot is shown in Fig. 70. It is seen to be visually linear, and extrapolates to $\mu = 18.7 \pm 0.2$. Note that this linearity implies a stretched-exponential term with exponent $1/2$. Linear intercepts, which eliminate the competing $O(1/n)$ term, allow this estimate to be sharpened to $\mu = 18.65 \pm 0.1$. A variety of other methods were also employed to estimate μ. These were all consistent, and gave slightly more precision. We combine these various estimates of μ to give the final estimate $\mu = 18.66 \pm 0.05$.

Assuming $\sigma = 1/2$, one can fit sequences of four successive ratios to the asymptotic form given by eqn. (23), and also fit four successive coefficients to the asymptotic form eqn. (20).

From the fit to the ratios, we find $\mu = 18.66 \pm 0.05$, and $\sigma \log \mu_1 = -1.8 \pm 0.1$, so $\mu_1 = 0.027 \pm 0.006$.

From the fit to the logarithm of the coefficients we were unable to usefully estimate $\log C$. Both these methods gave an estimated result for the exponent g in the vicinity of -4. We expect $g = -4 \pm 1$.

We can directly estimate σ assuming the value of μ by two methods, as described above. The first estimator is given by eqn. (15), the second by calculating the gradient of the log-log plot obtained from eqn. (16). One can also estimate the value of σ without any estimate of μ, by calculating the local gradient of the log-log plots of the two estimators given by eqn. (17) and eqn. (18). Both pairs of plots give results totally consistent with our previous estimate $\sigma = 1/2$.

We therefore conclude that $s_n(53241) \sim C \cdot \mu^n \cdot \mu_1^{n^\sigma} \cdot n^g$, with $\mu = 18.66 \pm 0.05$, $\sigma = 1/2$, $\mu_1 = 0.027 \pm 0.006$, and $g = -4 \pm 1$. We give no estimate of the amplitude C.

Lower bounds

Assuming that the coefficients form a Stieltjes moment sequence, the consequent log-convexity gives the bound $\mu(53241) \geqslant 11.8339$. If the 100 predicted coefficients are believed, this improves the bound to $\mu(53241) \geqslant 15.5411$.

Constructing the continued fraction representation from the exact coefficients, (see Theorem 1 above), as in the previous PAP, then one finds $\mu(53241) \geqslant 15.4445$.

This sequence of lower bounds can also be extrapolated against $1/n^{2/3}$, shown in Fig. 71, and results in an estimate of $\mu \approx 18.7$, consistent with that obtained by the direct analysis of the original, extended series.
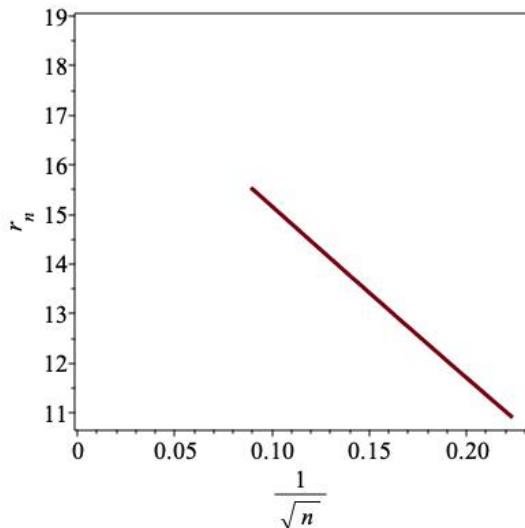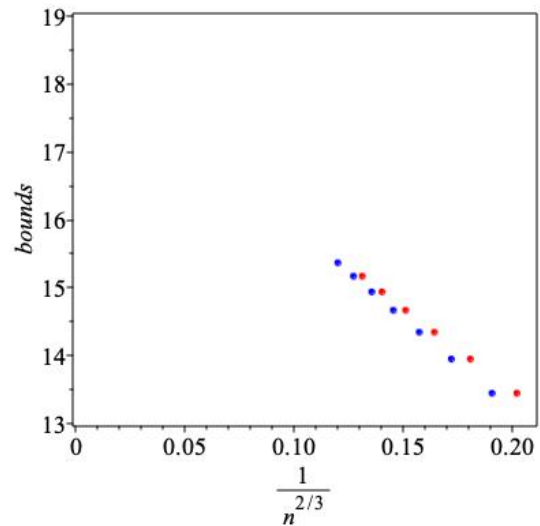
Figure 70: $Av(53241)$ ratios vs. $1/\sqrt{n}$.

Figure 71: Stieltjes bounds on μ for $Av(53241)$.

Av(53421)

This series was known up to, and including, terms of order x^{14}, given in the OEIS as sequence A256207. We have extended the series by twelve further terms. We have also extended the sequence of ratios, and coefficients, by 200 further terms, as described above.

The ratios, when plotted against $1/n$, display curvature, which disappears when the ratios are plotted against $1/n^{1/2}$. This implies a singularity structure with a stretched exponential term. The ratio plot against $1/\sqrt{n}$ is shown in Fig. 72. It appears to be linear, and extrapolates to $\mu = 19.4 \pm 0.2$. This linearity implies a stretched-exponential term with exponent $\sigma = 1/2$.

However, we can get a much more precise estimate of μ in this case, as Bóna in [8] points out that, using techniques from [7] one can prove that $\mu(53421) = (1 + \sqrt{\mu(Av(1324))})^2 \approx 19.4092$. See also [1]. Here we have used the estimate $\mu(Av(1324)) \approx 11.598$ given in [11]. In that paper, it is pointed out that $9 + 3\sqrt{3}/2 = 11.598\ldots$. If that surd is the exact value of $\mu(Av(1324))$, it would follow that $\mu(53421) = 10 + \sqrt{36 + 6\sqrt{3}} + 3\sqrt{3}/2 = 19.409265890507264\ldots$. For our subsequent analysis, it is immaterial which of these two estimates of μ we use.

Given this more precise estimate of μ than we have had in most other cases, we can get useful estimates of the other critical parameters. We fit to

$$s_n(53421) = c_n \sim C \cdot \mu^n \cdot \mu_1^{\sqrt{n}} \cdot n^g.$$

Then

$$\log c_n - n \log \mu \sim \log C + \sqrt{n} \log \mu_1 + g \log n.$$

We can fit successive triples of coefficients to this equation, giving a linear system the solution of which gives estimators of the three unknowns, C, $\log \mu_1$ and g. The results

of these fits are shown in Figs. 73, 74, 75 below. Visually extrapolating these gives the estimates $\log C = 2 \pm 0.3$, $\log \mu_1 = -3.13 \pm 0.03$, and $g = -4.0 \pm 0.5$. This gives $C = 7.4 \pm 2$, $\mu_1 = 0.044 \pm 0.002$, and $g = -4.0 \pm 0.5$.
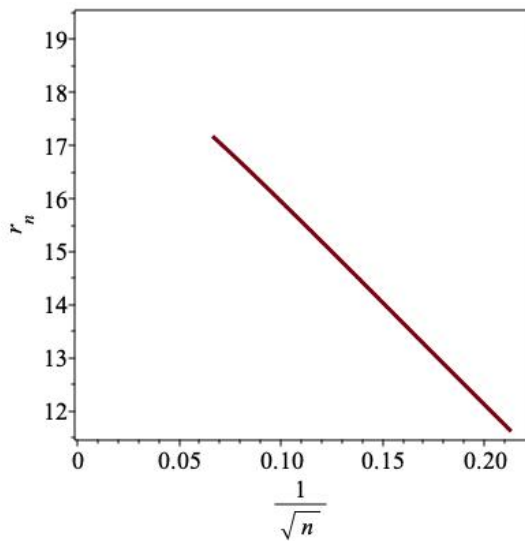

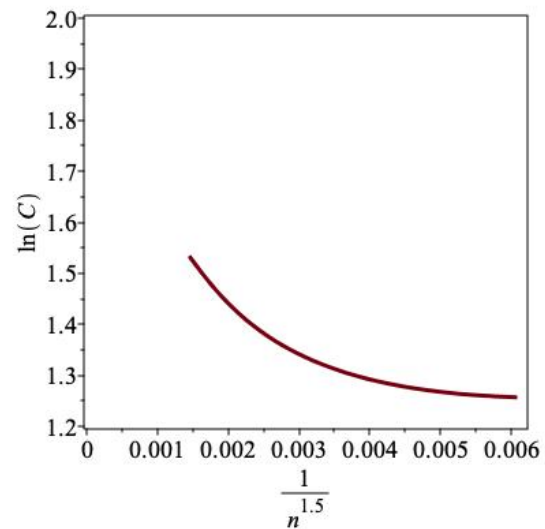Figure 72: $Av(53421)$ ratios vs. $1/\sqrt{n}$.

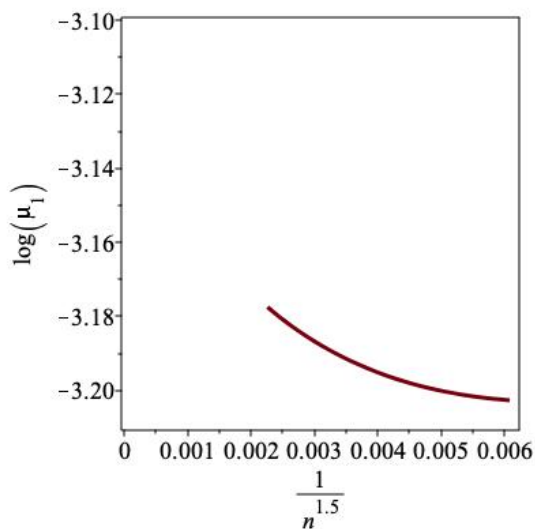Figure 73: Estimators of $\log(C)$ vs. $1/n^{5/2}$.

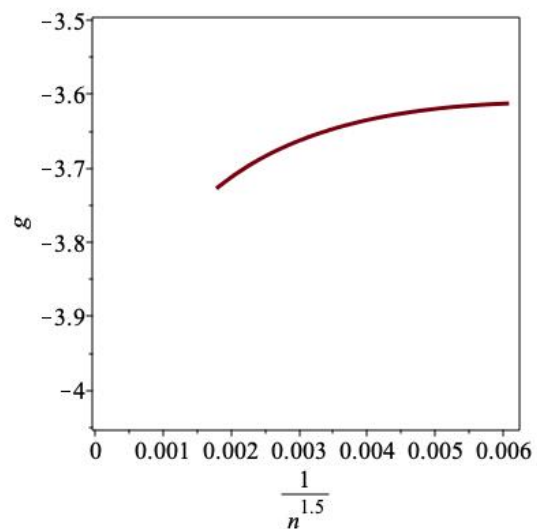Figure 74: Estimators of $\log(\mu_1)$ vs. $1/n^{3/2}$.

Figure 75: Estimators of g vs. $1/n^{3/2}$.

We therefore conclude that $s_n(53421) \sim C \cdot \mu^n \cdot \mu_1^{n^\sigma} \cdot n^g$, with $\mu \approx 19.4092$, $\sigma = 1/2$, $C = 7.4 \pm 2$, $\mu_1 = 0.044 \pm 0.002$, and $g = -4.0 \pm 0.5$.

Lower bounds

Assuming that the coefficients form a Stieltjes moment sequence, the consequent log-convexity gives the bound $\mu(53421) \geqslant 12.4079$. If the 200 predicted coefficients are believed, this improves the bound to $\mu(53421) \geqslant 17.1769$.

Constructing the continued fraction representation from the exact coefficients, (see Theorem 1 above), as in the previous PAP, then one finds $\mu(53421) \geqslant 16.3053$.

This sequence of lower bounds can also be extrapolated against $1/n^{2/3}$, and results in an estimate of $\mu \approx 18.9$, a little lower than the known result.

Av(52341)

This series was known up to, and including, terms of order x^{14}, given in the OEIS as sequence A256208. We have extended the series by nine further terms. This was, computationally, the most demanding series to generate. With 2TB of memory, we could only get to $O(x^{23})$, with 15 hours of computing time, whereas with most other patterns we could get to $O(x^{26})$ with only 1TB memory and a similar amount of computing time. We have also extended the sequence of ratios and coefficients by 50 further terms as described above.

The ratios, when plotted against $1/n$, see Fig. 76, display considerable curvature, which is substantially reduced when the ratios are plotted against $1/n^{1/2}$, shown in Fig. 77. This again suggests a singularity structure with a stretched exponential term, similar to that observed for $Av(4231)$ PAPs [11]. This is not surprising, as this pattern contains the pattern 4231. Extrapolating the ratios, we estimate $\mu \approx 24.6 \pm 0.5$. Next, we calculated the linear intercepts $l_n \equiv n \cdot r_n - (n-1) \cdot r_{n-1}$ which eliminate the $O(1/n)$ term in the ratios. The results are shown in Fig. 78, and which we extrapolate to $\mu \approx 24.8 \pm 0.5$.
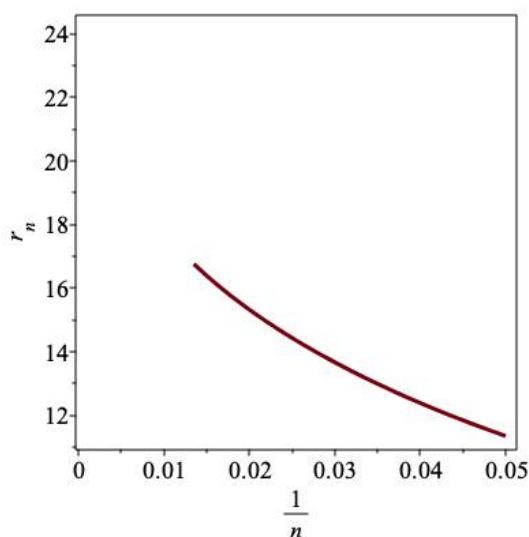

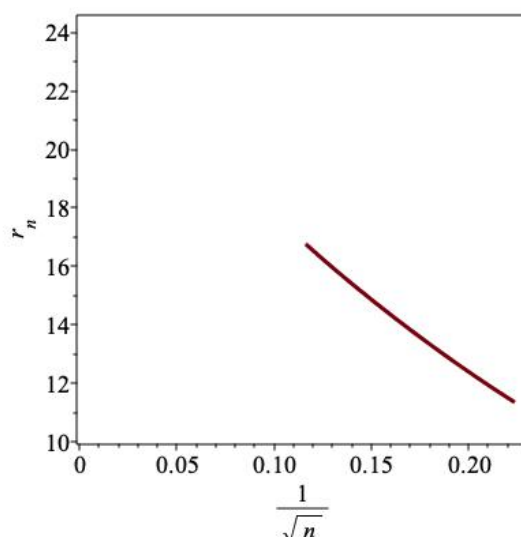Figure 76: $Av(53421)$ ratios vs. $1/n$.

Figure 77: $Av(53421)$ ratios vs. $1/\sqrt{n}$.

Using the methods discussed in the analysis of previous patterns, we have estimated

the value of the stretched-exponential exponent σ. We show in Fig. 79 estimators of σ obtained without assuming the value of μ. It can be seen that they are quite consistent with the value $1/2$, so we feel confident suggesting that $\sigma = 1/2$ exactly.
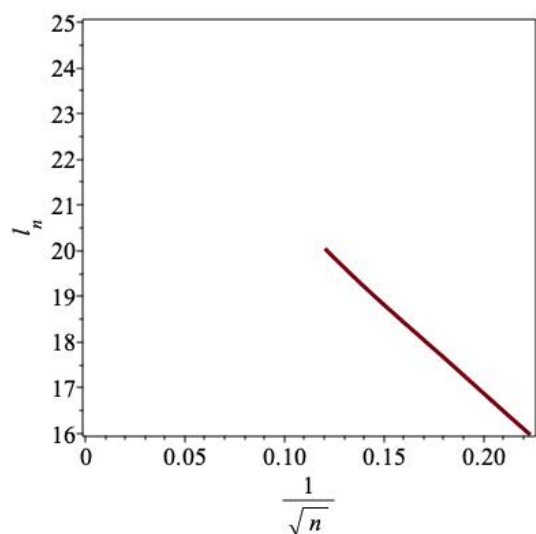

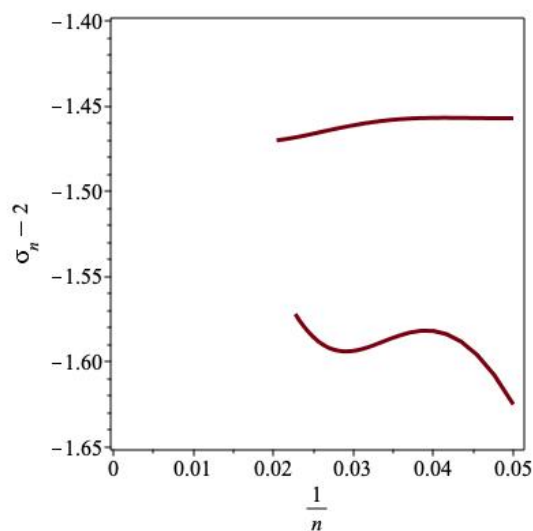Figure 78: Linear intercepts of $Av(53421)$ vs. $1/\sqrt{n}$.

Figure 79: Estimators of σ for $Av(53421)$ vs. $1/n$.

Assuming $\sigma = 1/2$ have also estimated the value of μ by fitting successive quadruples of ratios, $r_{k-2}, r_{k-1}, r_k, r_{k+1}$ to the expected asymptotic form (10), which gives estimators of μ as shown in Fig. 80, which while difficult to extrapolate, is not inconsistent with previous estimates. This fit also gives estimators of the growth constant μ_1, more precisely of $\mu \cdot \log \mu_1 / 2$, which extrapolates to a value around -80, from which one concludes that $\mu_1 \approx 0.0016$. We can also estimate the growth constant μ_1 by plotting $(r_n/\mu - 1) \sim \log(\mu_1)/2$ against $1/\sqrt{n}$, which extrapolates to -3.3 ± 0.1, so that $\mu_1 = 0.0014 \pm 0.0003$.

We therefore conclude that $s_n(52341) \sim C \cdot \mu^n \cdot \mu_1^{\sqrt{n}} \cdot n^g$, with $\mu = 24.8 \pm 0.5$, $\sigma = 1/2$, $\mu_1 \approx 0.0015$. We give no estimate of the exponent g or the amplitude C.

Lower bounds

Assuming that the coefficients form a Stieltjes moment sequence, the consequent log-convexity gives the bound $\mu(52341) \geqslant 12.1999$. If the 50 predicted coefficients are believed, this improves the bound to $\mu(52341) \geqslant 16.7641$.

If one constructs the continued fraction representation from the exact coefficients, (see Theorem 1 above), as in the previous PAP, then by the same construction one finds $\mu(52341) \geqslant 15.7310$.

This sequence of lower bounds can also be extrapolated against $1/n^{2/3}$, see Fig. 81 and results in an estimate of μ consistent with that obtained by the direct analysis of the original, extended series.
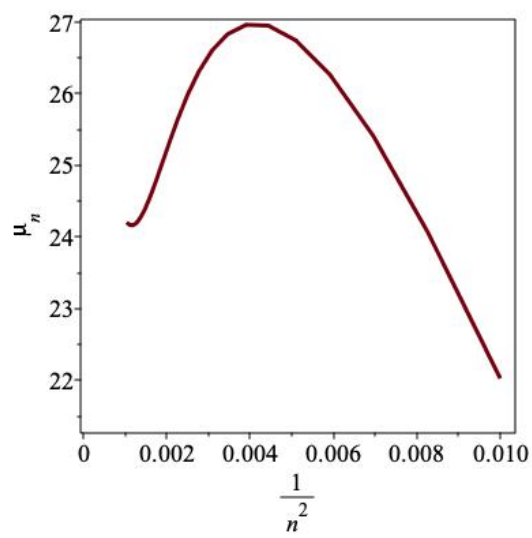
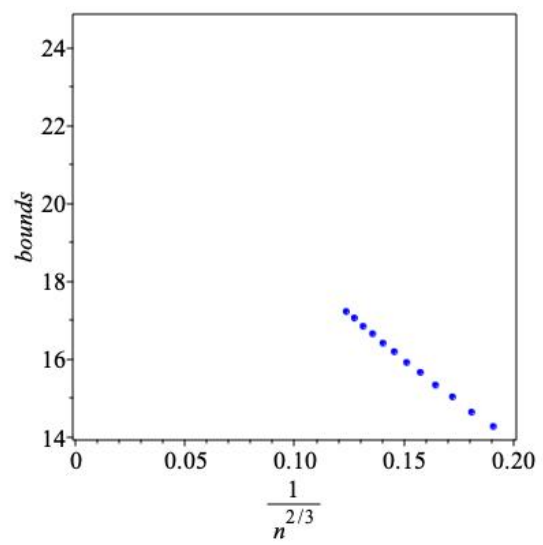Figure 80: Estimators of μ for $Av(52341)$ vs. $1/n^2$.

Figure 81: Bounds on μ for $Av(52341)$ vs. $1/n^2/3$.